



## 저작자표시-비영리-변경금지 2.0 대한민국

이용자는 아래의 조건을 따르는 경우에 한하여 자유롭게

- 이 저작물을 복제, 배포, 전송, 전시, 공연 및 방송할 수 있습니다.

다음과 같은 조건을 따라야 합니다:



저작자표시. 귀하는 원저작자를 표시하여야 합니다.



비영리. 귀하는 이 저작물을 영리 목적으로 이용할 수 없습니다.



변경금지. 귀하는 이 저작물을 개작, 변형 또는 가공할 수 없습니다.

- 귀하는, 이 저작물의 재이용이나 배포의 경우, 이 저작물에 적용된 이용허락조건을 명확하게 나타내어야 합니다.
- 저작권자로부터 별도의 허가를 받으면 이러한 조건들은 적용되지 않습니다.

저작권법에 따른 이용자의 권리는 위의 내용에 의하여 영향을 받지 않습니다.

이것은 [이용허락규약\(Legal Code\)](#)을 이해하기 쉽게 요약한 것입니다.

[Disclaimer](#)

# **Differential Expression of A MicroRNA in The Development of Dendritic Cells**



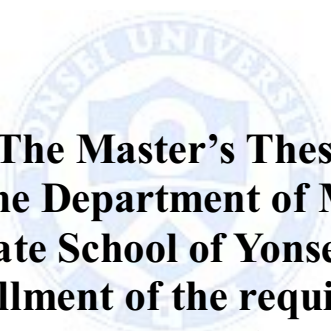
**Sun M Han**

**Department of Medical Science**

**The Graduate School, Yonsei University**

# **Differential Expression of A MicroRNA in The Development of Dendritic Cells**

**Advised by Professor Chae Gyu Park**



**The Master's Thesis  
submitted to the Department of Medical Science,  
the Graduate School of Yonsei University  
in partial fulfillment of the requirements for the  
degree of  
Master of Medical Science**

**Sun M Han**

**December 2015**

**This certifies that the Master's Thesis of  
Sun M Han is approved.**

**박채규**

---

**Thesis Supervisor: Chae Gyu Park**

**김형표**

---

**Thesis Committee Chair: Hyoung-Pyo Kim**

**황기철**

---

**Thesis Committee Member: Ki-Chul Hwang**

**The Graduate School  
Yonsei University**

**December 2015**

## **Acknowledgements**

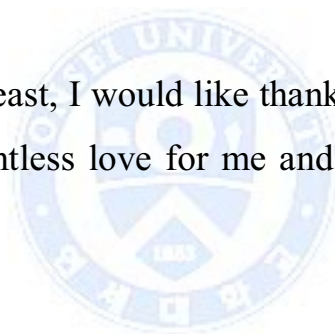
I would like to express my foremost gratitude to my advisor, Professor Chae Gyu Park. Not only did Professor Park accept me to his laboratory mid-way through my Master's degree from a different department, he immediately got me enthralled with his passion for and knowledge of immunology. He provided a grand learning atmosphere and allowed me to bridge my previous study with the concepts that he was exploring. His enthusiasm for research raised my love for science and motivated me to elucidate my curiosities with great intrigue during my graduate experience. I am indebted to you for your excellent supervision and for the immeasurable inspiration and motivation you have given me.

I would also like to thank Professor Hyoungh-Pyo Kim and Professor Ki-Chul Hwang for their time and input as committee members for this thesis. Their varying and in-depth perspectives have stimulated my work and have helped me strengthen my research. I would like to further thank Professor Ki-Chul Hwang for his supervision during my initial study at Yonsei and for helping me make a transition with a heightened zeal for science.

My sincere appreciation goes to Dr. Onju Ham for her individual contribution and collaboration on this research and to Dr. Hye Young Na for not only helping me in all aspects of this thesis but also for comprehensively enforcing my technique and knowledge since joining this laboratory.

I would also like to thank my colleagues Moah Sohn, Seul Hye Ryu, Wanho Choi, and Hyunju In for their vitalizing camaraderie and for always providing an enticing atmosphere for research.

And last but not least, I would like thank my father, mother, and brother for their relentless love for me and their support in all my endeavors.



Sincerely,  
Sun M. Han

# TABLE OF CONTENTS

<b>ABSTRACT</b> .....	1
<b>I. INTRODUCTION</b> .....	3
<b>II. MATERIALS AND METHODS</b> .....	13
2.1 Mice.....	13
2.2 Bone marrow extraction .....	13
2.3 Splenocyte preparation .....	13
2.4 Cell, antibodies, and reagents .....	14
2.5 Production of Flt3L from Chinese hamster ovary cells .....	15
2.6 Flow cytometry .....	16
2.7 RNA isolation and real-time PCR.....	16
2.7.1 RNA isolation .....	16
2.7.2 TaqMan™ real-time PCR.....	16
2.7.3 SYBR® Green real-time PCR .....	17
2.8 Luciferase activity assay.....	18
2.9 miR-124 mimic/inhibitor transfection.....	18
2.10 Culture of CDPs and miR-124 transfection.....	19
2.11 Statistical analyses .....	19

<b>III. RESULTS</b>	20
3.1 Candidate miRNAs related to DC development	20
3.2 miR-124 is outstandingly expressed in DC subset	26
3.3 miR-124 might directly regulate Tcf4 activity	29
3.4 Bone marrow cells differentiate into distinct subsets upon culture with Flt3L	32
3.5 pre-DCs cultured <i>in vitro</i> with Flt3L show high expression of miR-124	39
3.6 cDC1 cells in BM show high expression of miR-124	45
3.7 cDC1 cells in spleen show high expression of miR-124	49
3.8 All three miR-124 precursor transcripts contribute to miR-124 expression in cDC1 cells	51
3.9 Overexpression of miR-124 causes significant changes to <i>in vitro</i> -cultured DC populations	53
<b>IV. DISCUSSION</b>	55
<b>V. CONCLUSION</b>	58
<b>REFERENCES</b>	59
<b>ABSTRACT (IN KOREAN)</b>	62
<b>PUBLICATION LIST</b>	64



## LIST OF FIGURES

<b>Figure 1</b>	Characteristics of mature DC subsets .....	6
<b>Figure 2</b>	Schematic view of DC ontogeny and development of distinct subsets .....	7
<b>Figure 3</b>	DC fate is dependent on Flt3L and GM-CSF.....	9
<b>Figure 4</b>	Identification of candidate miRNAs that potentially target the transcript of transcription factors in DC development.....	21
<b>Figure 5</b>	Initial expression screening of candidate miRNAs .....	27
<b>Figure 6</b>	miR-124 directly regulates 3'UTR of Tcf4.....	30
<b>Figure 7</b>	<i>In vitro</i> generation of pre-DCs by culture of BM cells with Flt3L .....	33
<b>Figure 8</b>	<i>In vitro</i> generation of pDCs by culture of BM cells with Flt3L .....	36
<b>Figure 9</b>	<i>In vitro</i> generation of cDCs by culture of BM cells with Flt3L .....	37
<b>Figure 10</b>	Isolation of BM CS subsets generated <i>in vitro</i> and miR-124 expression .....	41
<b>Figure 11</b>	Isolation of steady-state BM DC subsets and miR-124 expression .....	47
<b>Figure 12</b>	Isolation of pre-DC subpopulations in steady-state BM and miR-124 expression.....	48
<b>Figure 13</b>	Isolation of steady-state spleen DC subsets and miR-124 expression .....	50

<b>Figure 14</b> Contribution of the three miR-124 precursors to miR-124 expression in DC subset .....	52
<b>Figure 15</b> Isolation of steady-state BM DC subsets and miR-124 expression .....	54



# **Differential Expression of A MicroRNA in The Development of Dendritic Cells**

**Sun M Han**

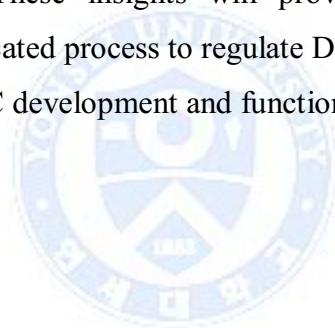
*Department of Medical Science  
The Graduate School, Yonsei University*

**(Advised by Professor Chae Gyu Park)**

## **Abstract**

Dendritic cells (DCs) are professional antigen-presenting cells that sample and present antigens to naïve T lymphocytes, which is necessary for the subsequent antigen-specific T-cell immune responses. DCs exist in a range of distinct subpopulations including plasmacytoid DCs (pDCs) and classical DCs (cDCs), with the latter consisting of the cDC1 and cDC2 lineages. Although the roles of DC-specific transcription factors across the DC subsets have become understood, the posttranscriptional mechanisms that regulate DC development are yet to be elucidated. MicroRNAs (miRNAs) are pivotal posttranscriptional regulators of gene expression in a myriad of biological processes, but their contribution to the immune system is just beginning to surface. To identify miRNAs possibly involved in DC development and function, we screened for the expression of candidate miRNAs that target the 3'UTR of relevant transcriptional factors from our in-house probe collection. We identified miR-124 which was able to target and directly regulate the expression of transcription factor Tcf4, a gene known to be critical for the development and homeostasis of pDCs. We then utilized an *in vitro* model for DC development using bone marrow (BM) culture with Flt3L, where miR-124

was exceedingly expressed in pre-cDCs relative to the mature DC subsets (pDC, cDC1, and cDC2). Meanwhile, the *in vivo* expression profiling of the subsets isolated from BM showed that miR-124 was outstandingly expressed in CD24<sup>+</sup> cDC1s compared to DC precursors, pDCs, and CD172α<sup>+</sup> cDC2s. We also investigated the effects of miR-124 mimic or inhibitor exaggeration on DC development to examine the phenotypic changes influenced by miR-124. Transfection of miR-124 mimic into BM common DC progenitors (CDP) followed by culture with Flt3L caused significant changes in resulting mature DC populations, where large decrease of a previously unrecognized DC subset was observed. These results imply mechanistic involvement of miR-124 in DC subset differentiation. These insights will provide further evidence into understanding a sophisticated process to regulate DC ontogeny where miR-124 plays a crucial role in DC development and function.



---

Key words: Dendritic cells, lineage development, microRNA, posttranscriptional regulation

# **Differential Expression of A MicroRNA in The Development of Dendritic Cells**

**Sun M Han**

*Department of Medical Science  
The Graduate School, Yonsei University*

**(Advised by Professor Chae Gyu Park)**

## **I. Introduction**

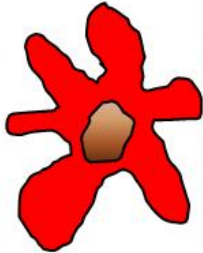



Dendritic cells (DCs) are antigen-presenting cells (APCs) found in lymphoid organs as well as in tissue, especially those with interfaces exposed to the external environment. They essentially act as specialized sentinel cells that sample their local environment for antigens to present to naïve T lymphocytes, which is solely necessary for the subsequent antigen-specific T-cell activation and induction of immune responses.<sup>11</sup> When they were first described by Ralph Steinman in 1973, immunologists widely believed macrophages to be the main antigen-presenting cells in the immune system. While first deemed superfluous and their antigen-presenting capacity overshadowed by the physiological predominance of macrophages, dendritic cells have since been established to be the main APCs in our body and to play a crucial role in the innate and adaptive response to infection as well as in maintaining self-tolerance.<sup>1</sup> Accordingly, DCs have garnered increasing scrutiny and their pivotal role in the orchestration of the innate and adaptive immune responses have made it an unavoidable target in studying disease and in understanding the human immune system.

Many varieties of DC subpopulations have been described in both humans and mouse with each characterized by particular locations, phenotypic morphologies, and functions. In essence, DCs consist of a range of functionally distinct subsets that can be identified by their differential expression of particular surface markers.<sup>16</sup> The DC subsets prevalent in the steady state include migratory DCs such as Langerhans cells (LCs), plasmacytoid DCs (pDCs), and lymphoid tissue-resident classical DCs (cDCs).<sup>16</sup> LCs are generally present in the skin and mucosa, while lymphoid tissue-resident pDCs and cDCs can be found in the spleen and lymph nodes. pDCs are PDCA-1<sup>+</sup>, B220<sup>+</sup> and mainly function in producing type I interferons. The lymphoid tissue-resident cDCs further segregate into different subtypes including CD8 $\alpha$ <sup>+</sup>, CD24<sup>+</sup>, CD11b<sup>-</sup> cDC1, which efficiently cross-present antigens to CD8<sup>+</sup> T cells and principally produce interleukin-12 p70 (IL-12p70), and CD8  $\alpha$ <sup>-</sup>, CD11b<sup>+</sup>, CD172 $\alpha$ <sup>+</sup> cDC2, which present Class II restricted antigens to CD4<sup>+</sup> T cells.<sup>4, 12, 14, 21</sup> Also, more DC subtypes develop upon infection or inflammation such as the monocyte-derived inflammatory DCs (MoDCs).<sup>14</sup> The common mouse and human mature DC subsets and the markers they carry along with their major functions are described in the chart in **Figure 1**. Immunologists have thus far used these phenotypic distinctions to characterize and attribute varying functions and physiological involvements to particular populations.

The development of DCs to their respective subset counterparts arise through a multistage process. Like all other immune cells, DCs develop from hematopoietic stem cells (HSCs) in the bone marrow (BM). HSCs differentiate into the myeloid progenitor (MP), which subsequently differentiates into the monocyte and DC progenitor (MDP) and then into the common DC progenitor

(CDP).<sup>16, 20</sup> CDPs develop into pre-DCs and pDCs and then egress from the bone marrow to the periphery. These cells seed peripheral secondary lymphoid tissues and non-hematopoietic tissues and ultimately mature into either cDCs or pDCs.<sup>12, 14</sup> A comprehensive portrayal is shown in **Figure 2**.



Myeloid Classical DCs			
cDC1		cDC2	
<b>Human</b> CD141 <sup>+</sup> CLEC9A <sup>+</sup> CD11b <sup>-</sup> XCR1 <sup>+</sup> TLR3 <sup>+</sup> FLT3 <sup>+</sup> CD11c <sup>low</sup>		<b>Mouse</b> CD11c <sup>+</sup> CD8α <sup>+</sup> (lymphoid) CD103 <sup>+</sup> (non-lymphoid) CLEC9A <sup>+</sup> CD11b <sup>-</sup> XCR1 <sup>+</sup> TLR3 <sup>+</sup> FLT3 <sup>+</sup> CD24 <sup>+</sup> CD205 <sup>+</sup>	
<ul style="list-style-type: none"><li>• Cross-presentation</li><li>• MHC class I-restricted antigens</li><li>• <b>CD8 T cell responses</b></li></ul>		<ul style="list-style-type: none"><li>• MHC class II-restricted antigens</li><li>• <b>CD4 T cell responses</b></li></ul>	
Non-Classical DCs			
Monocyte-derived DC		Plasmacytoid DC	
<b>Human</b> CD14 <sup>+</sup> CD11b <sup>+</sup> CD11b <sup>-</sup> CX3CR1 <sup>+</sup> CD209 <sup>+</sup>		<b>Mouse</b> CD11b <sup>+</sup> CX <sub>3</sub> CR1 <sup>+</sup> (intestine) CLEC9A <sup>+</sup> CD206 <sup>+</sup> CD209 <sup>+</sup>	
<ul style="list-style-type: none"><li>• TNF</li><li>• iNOS</li><li>• Bacterial antigens</li><li>• Secondary immune responses</li><li>• <b>Inflammatory responses</b></li></ul>		<ul style="list-style-type: none"><li>• <b>Type I interferons</b></li><li>• Durable memory responses</li></ul>	

**Figure 1. Characteristics of mature DC subsets.** Representative cDC1, cDC2, pDC, and monocyte-derived DC markers and function.



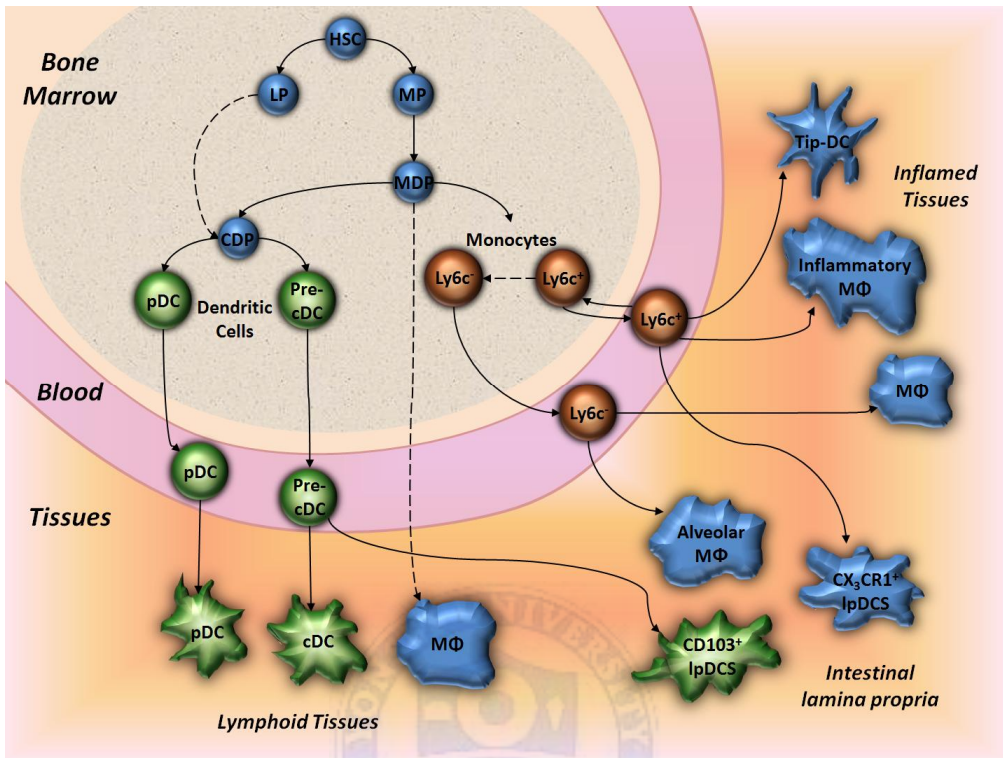


**Figure 2. Schematic view of DC ontogeny and development of distinct subsets.** DC subsets with distinct functions and markers are generated from BM progenitor cells and the development of DCs to their respective subset counterparts arise through a multistage process.

Development of DCs from their progenitor cells can be replicated *in vitro* with various culture conditions. Culture of DC progenitors with the growth factor fms-like tyrosine kinase-3 ligand (Flt3L) produces a heterogeneous population containing both cDCs and pDCs, which are equivalent to their *in vivo* counterparts with respect to cell surface marker expression, transcription factor reliance, cytokine production, receptor molecule expression, and antigen-presenting ability to T lymphocytes.<sup>11, 17</sup> Principally, the Flt3L-culture borne cells correspond to steady state populations.<sup>8, 11</sup> DC development can also be modeled by culturing DC progenitors with granulocyte macrophage colony-stimulating factor (GM-CSF). GM-CSF induces DCs that are more granular and produce more inflammatory mediators, such as tumor necrosis factor- $\alpha$  and interleukin-10.<sup>23</sup> In essence, they are the *in vitro* equivalents of inflammatory MoDCs, and the generation of MoDCs from the *in vitro* culture of murine BM cells with GM-CSF and IL-4 has been extensively described.<sup>11</sup> The presence of Flt3L or GM-CSF incites the progenitor cells to differentiate into their mature counterparts. The general ontogeny of the DC subpopulations is portrayed in **Figure 3**. Myeloid progenitor (MP) cells differentiate into macrophage-DC progenitors (MDP) in the BM. In the presence of GM-CSF, MDPs differentiate into monocytes and then into inflammatory DCs. In the presence of Flt3L, MDPs have the capacity to differentiate into common-DC progenitor (CDP). CDPs further differentiate into pDCs or into pre-DCs that ultimately generate the cDC lineages. In essence, these *in vitro* culture systems that effectively simulate *in vivo* developments have allowed a grander accessibility to study the distinct functions of the varying subtypes.

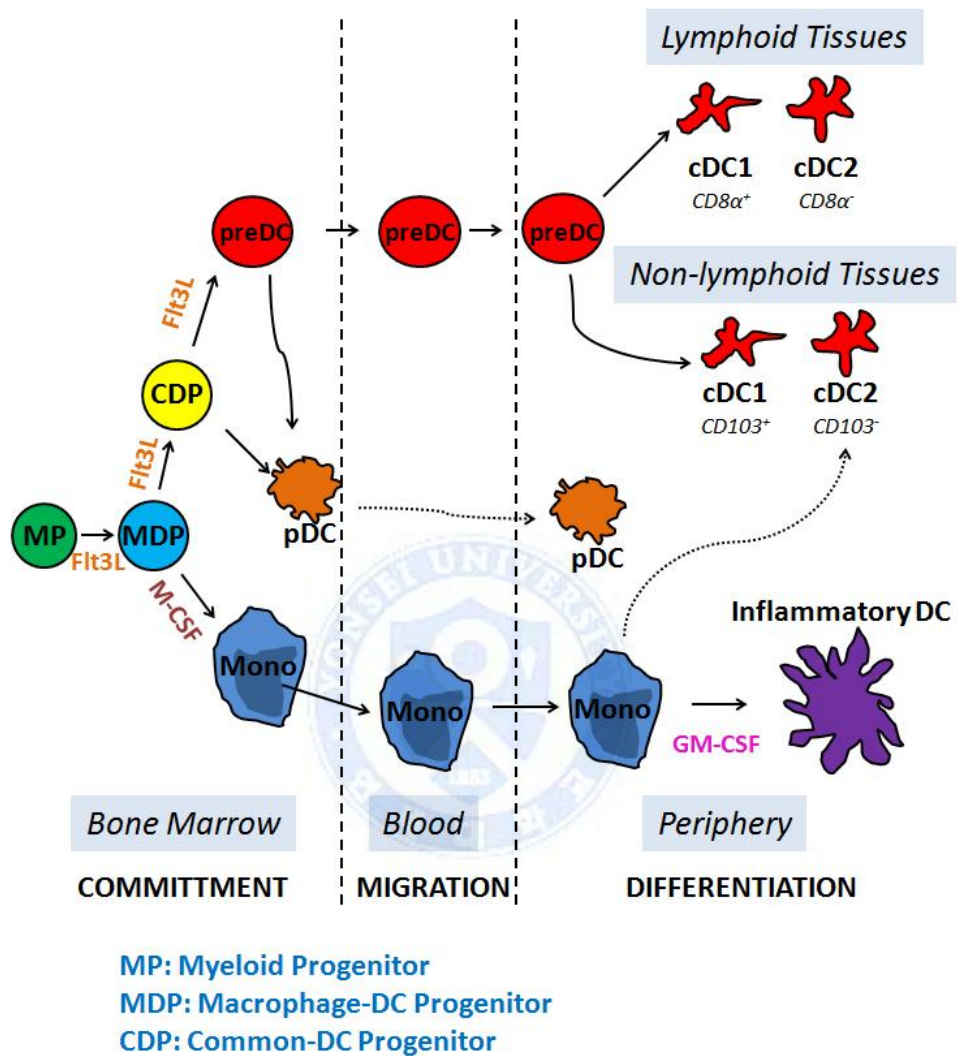


**Figure 3. DC fate is dependent on Flt3L and GM-CSF.** Schematic showing the multistage process of DC development from BM progenitors to mature DC subsets depending on the inducing factor.

In light of these investigatory advances, the roles of transcription factors in DC development and their dynamic profiles across the subsets have become well understood. As for one, the transcription factor PU.1 has been described to play a role in the development of all DCs.<sup>15</sup> Meanwhile, signal transducer and activator of transcription 5 (STAT5) is known to drive the development of cDCs in favor of pDCs through the inhibition of transcription factor interferon regulatory factor 8 (IRF8), whereas immunoglobulin transcription factor 2 (TCF4) is known to drive pDC development over cDC by directly activating Irf8 and other pro-pDC transcription factors such as SpiB.<sup>3, 6, 15</sup> As such, a comprehensive group of transcription factors and their involvement in the particular stages of DC development have been mapped. In contrast to these transcriptional mechanisms though, posttranscriptional mechanisms that regulate DC development are less well understood. With the heterogeneity of subsets and wide-ranging function of DCs, the natural question arises on how DC differentiation and development is regulated besides the orchestration of growth factors and transcription factors. Recently, increasing evidence has shown that microRNAs (miRNAs) play an important role in fine-tuning DC development and function.

miRNAs are an evolutionarily conserved class of short, endogenous, non-coding RNAs about 19~23 nucleotides long that regulate protein synthesis by targeting the complementary 3' untranslated region (UTR) of messenger RNAs (mRNAs) for translational repression and degradation.<sup>8, 10</sup> miRNA biogenesis begins with the transcription of a miRNA gene, which generates a primary miRNA transcript (pri-miRNA) through RNA polymerase II. The pri-miRNA then bind DiGeorge syndrome critical region gene 8 (DGCR8) and the stem-loop structure is subsequently recognized and cleaved by the RNase III enzyme of endonuclease Drosha to release the hairpin pre-miRNA transcripts.<sup>6</sup>

These transcripts are exported from the nucleus via Exportin-5, and the structures are further processed by Dicer to remove the loop and generate a miRNA duplex. A strand of the duplex is then segregated to give a mature 19- to 23bp miRNA species which is incorporated into the RNA-induced silencing complex (RISC) assembly containing the Argonaute (Ago) protein. The assembly ultimately targets mRNAs for translational repression or degradation. A key characteristic of miRNAs is that each has the ability to inhibit a myriad of mRNAs, and each mRNA can be targeted by many miRNAs.<sup>8, 10, 23</sup> This sketches a complex network of miRNAs surrounding DC development.

miRNAs have been shown to be vital in controlling many processes within the immune system.<sup>1, 10</sup> Their involvement in regulating T- and B-lymphocyte development has been established of late and their wide-ranging roles in cell differentiation, homeostasis, cytokine responses, and interactions with pathogens and tolerance induction among others have been described.<sup>8, 9, 23, 24</sup> More recent progressions have attempted to describe the role of miRNAs in DC development. Several miRNAs have been specifically attributed to the direct regulation of certain DC functions and more have been identified by the mapping of dynamic profiles across the subsets.<sup>10, 23</sup> More specifically, recent research has emphasized the requirement of miRNAs in DC lineage commitment from BM progenitors and for the development of certain subsets.<sup>8</sup> Cluster analyses across isolated subsets have shown a differential expression of miRNA throughout the developmental process of murine DC.<sup>13, 23</sup> In a particular study, Su *et al.*, used next-generation deep sequencing to demonstrate that 391 miRNA were differentially expressed during DC differentiation.<sup>24</sup> For example, mir-123 and miR-147 were highly expressed in both immature and mature subsets but not in HSCs.<sup>10</sup> These distinct miRNA

profiles and indications of miRNA involvement can also be observed among DC subsets and linked to particular transcription factors and functional properties.<sup>10, 13</sup> Immunologists have subsequently used knockout and overexpression studies to identify miRNAs along with corresponding transcription factors and their involvement in the development of particular subset populations as well as their affect on regulating DC homeostasis, cytokine profiles, and immune response induction capabilities among others.<sup>8-10, 13</sup> Mildner *et al.* observed that miR-125, let-7 and miR-21 were differentially expressed throughout pDCs, CD8 $\alpha^+$  cDCs, and CD4 $^+$  cDCs.<sup>13</sup> In a more particular example, Zhou *et al.* recently described that miRNA-146a and -146b regulate the apoptosis and cytokine production of moDCs by targeting TRAF6 and IRAK1 proteins.<sup>18</sup>

This increasing body of literature highlights the importance of specific miRNAs in DC development and regulation of their functional capacities. Like such, recent efforts have started to uncover the vast network of miRNAs that manipulate the biogenesis and mechanics of DCs; however, current knowledge is merely at the tip of the iceberg and though these studies have given such insight and building curiosity on the topic, the role of miRNAs in DC development and function remain largely elusive. Given the unique role of DCs in linking the innate and adaptive immune system, understanding how miRNAs affect DC function and development may be critical for understanding diseases and the immune system as a whole as well as providing insights into a novel target for therapeutic use and clinical application.

## **II. Materials and Methods**

### **2.1 Mice**

All experimental procedures for animal studies were approved by the Institutional Animal Care and Use Committee (IACUC) of Yonsei University College of Medicine. C57BL/6 mice were purchased from Orient Laboratories (Seongnam, Korea) and sacrificed at 6 to 8 weeks of age. CD45.1 and CD45.2 mice (all congenic on the C57BL/6 background) for transfection experiments were purchased from The Jackson Laboratory (Bar Harbor, ME) and bred for use at 6 to 10 weeks of age. Only healthy male mice were used in this study. Mice were bred at the Department of Laboratory Animal Resources at the Avison Biomedical Research Center of Yonsei University in specific pathogen-free conditions.

### **2.2 Bone marrow extraction**

Mice were sacrificed by asphyxiation in a CO<sub>2</sub> chamber. The hindlegs of the mice were excised and BM was flushed from the femur and tibia with Dulbecco's modified Eagle's medium (DMEM; HyClone Laboratories, Logan, UT) in sterile conditions. The extraction was then passed through a 100µm Nylon cell strainer to make single-cell suspensions. The cells were then washed multiple times with DMEM.

### **2.3 Splenocyte preparation**

Mice were sacrificed and spleens of the mice were extracted. Whole splenocyte suspensions were prepared by cutting and mincing the extracted whole spleens, grinding up the spleens with frosted glasses in DMEM, and



then passing the cells through a strainer. Cells were washed multiple times with DMEM.

## **2.4 Cells, antibodies, and reagents**

Chinese hamster ovary (CHO) cells (CHO-S cells; Gibco, Life Technologies, Carlsbad, CA) were cultured in DMC7 medium composed of DMEM containing L-glutamine, high glucose, and pyruvate (HyClone) and 7% fetal bovine serum (FBS; HyClone) supplemented with 1x solutions of non-essential amino acids and antibiotic-antimycotic (HyClone). The aforementioned mouse primary cells were used directly for *steady-state* experiments or were cultured in various dilutions of Flt3L-conditioned medium produced in our lab as described in below for *in vitro* experiments. The following conjugated antibodies were purchased from BioLegend (San Diego, CA): APC-Cy<sup>TM</sup>7-conjugated anti-I-A/I-E, anti-CD11c, anti-B220/CD45R, anti-CD45, anti-Rat IgG2b  $\kappa$  Isotype Control; Alexa Fluor<sup>®</sup> 647-conjugated anti-CD117; APC-conjugated anti-B220/CD45R, anti-PDCA-1 (BST2, CD317), anti-CD135; PE-Cy<sup>TM</sup>7-conjugated anti-Ly6G, anti-CD3, anti-CD11c, anti-CD19, anti-Ter119, anti-DX5, anti-I-A/I-E, anti-NK1.1, anti-Gr-1, anti-Sca-1; PerCP-Cy<sup>TM</sup>5.5-conjugated anti-Ly6C, anti-CD11c, anti-CD24, anti-CD117, anti-CD172 $\alpha$  (Sirp $\alpha$ ); PE-conjugated anti-SiglecH, anti-CD11c, anti-CD115, anti-CD117, anti-CD135, anti-Armenian Hamster (AH) IgG Isotype Control; FITC-conjugated anti-CD172 $\alpha$ ; Alexa Fluor<sup>®</sup> 488-conjugated anti-Ly6C, anti-CD172 $\alpha$ , anti-PDCA-1, anti-CD24, anti-CD45.2; Brilliant Violet<sup>TM</sup> 421 (BV421)-conjugated anti-CD11c, anti-CD45.1, anti-CD45.2, anti-CD115, anti-AH IgG Isotype Control; biotin-conjugated anti-NK1.1, anti-DX5, anti Ter119, anti-Ly6G, anti-CD3, anti-CD19, anti-CD135. LIVE/DEAD<sup>®</sup> fixable dead cell stain kit (Life Technologies) and propidium



iodide (Roche, Indianapolis, IN) were purchased and used according to the manufacturer's instructions.

## **2.5 Production of Flt3L from Chinese hamster ovary (CHO) cells**

The cDNA of mouse Flt3L was cloned by RT-PCR of total splenic RNA from C57BL/6 mice, and was used to generate a construct encoding soluble FLAG and OLLAS tagged Flt3L, internal ribosomal entry site (IRES), and enhanced green fluorescence protein (EGFP), i.e., SFO.Flt3L-IRES-EGFP.<sup>19</sup> The GenBank accession number for the sequence for the extracellular domain of Flt3L is GU168042, and the IRES-EGFP sequence is from pIRES-EGFP plasmid (Clontech, Mountain View, CA). CHO cells were then transfected using Lipofectamine 2000 (Life Technologies), with a mammalian expression vector plasmid encoding SFO.Flt3L-IRES-EGFP under CMV promoter and a neomycin resistance gene, generated with the backbone of pEGFP-N1 (Clontech). CHO/Flt3L cell-lines stably expressing the SFO.Flt3L-IRES-EGFP were generated by the following steps: (i) treatment of transfectant CHO cells with G418 (1.5mg/ml) for 1 week; (ii) enrichment of EGFP-positive CHO cells with FACS Aria II cell sorter (BD Biosciences); (iii) generation of clonal cells by limiting dilutions of FACS-sorted EGFP-high CHO/Flt3L cells; and (iv) selection of CHO/Flt3L clones after testing both levels of EGFP expression by FACS and Flt3L secretion by anti-OLLAS Western blot.<sup>19</sup> Selected CHO/Flt3L cells were cultured in cell culture bags (LAMPIRE, Pipersville, PA) with DMC7 to produce CHO/Flt3L-conditioned medium.

## **2.6 Flow cytometry**

Single cell suspensions were prepared from the harvest of mouse organ tissues or cultures thereof, incubated with 2.4G2 (Fc blocker) hybridoma supernatant, and washed with FACS buffer. Then, each sample was incubated with the appropriate mixture of fluorochrome-conjugated monoclonal antibodies and live/dead staining dyes described above. Cells were incubated for 30 min at 4°C and then washed with FACS buffer (2% FCS, 2 mM EDTA, 0.001-0.1% sodium azide) twice prior to analysis with FACSVerse flow cytometer (BD Biosciences, San Diego, CA) or sorting with FACS Aria II cell sorter (BD Biosciences). Flow cytometric data were analyzed using FlowJo software (FlowJo, Ashland, OR).

## **2.7 RNA isolation and real-time PCR**

### **2.7.1 RNA isolation**

Total RNA was isolated from sorted cells from cultured or uncultured mouse primary cells using TRIzol® Reagent (Life Technologies). The SYBR® Green and TaqMan™ systems were used to detect gene expression.

### **2.7.2 TaqMan™ real-time PCR**

For miR-124 expression profiling, 100 ng of purified total RNA was used for reverse transcription (Taqman® MicroRNA Reverse Transcriptase Kit, Applied Biosystems, Foster City, CA). The resultant cDNA was used in combination with Taqman® MicroRNA Assays mmu-miR-124a and U6 control transcripts and Taqman® Universal Master Mix II for PCR according to the manufacturer's instructions. The mature mmu-miR-124a (mmu-miR-124-3p, MIMAT0000134) sequence is 5'-UAAGGCACGCGGUGAAUGCC - 3'. The amplification and detection of

products were performed in a Light Cycler 480 II (Roche) with an initial denaturation at 95°C for 10 min, followed by 40-60 cycles of amplification at 95°C for 15 s and 60°C for 60 s before cooling. The threshold cycle (Ct) of miR-124 expression was automatically defined, located in the linear amplification phase of the PCR, and normalized to the control U6 ( $\Delta C_t$  value). The relative difference in expression levels of miR-124 in the sorted cells ( $\Delta\Delta C_t$ ) was calculated and presented as the fold induction ( $2^{-\Delta\Delta C_t}$ ).

### 2.7.3 SYBR® Green real-time PCR

For pri-miR-124 and relevant transcription factor profiling, 100 ng of purified total RNA was used for reverse transcription (PrimeScript™ RT Reagent Kit, TaKaRa Bio Inc., Ohtsu, Japan). The resultant cDNA was used in combination with designed short oligonucleotides (Cosmo Genetech, Seoul, Korea) and SYBR® Premix Ex Taq II (TaKaRa) for PCR according to the manufacturer's instructions. The primers sequences for the transcription factors were designed and produced by Cosmo Genetech. The primer sequences for the precursor transcripts of mmu-miR-124 are as follows: pri-miR-124-1, 5'-GCCTCTCTCTCCGTGT-3' forward, 5'-CCATTCTTGGCATTCA-3' reverse; pri-miR-124-2, 5'-AGAGACTCTGCTCTCCGTGT-3' forward, 5'-CTCCGCTCTTGGCATTC-3' reverse; pri-miR-124-3, 5'-GGCTGCGTGTTACACAG-3' forward, 5'-ATCCCGCGTGCCTTA-3' reverse; GAPDH, 5'-ACAGTCCATGCCATCACTGCC-3' forward, 5'-GCCTGCTTCACCACCTTCTTG-3' reverse. The amplification and detection of products were performed in a Light Cycler 480 II (Roche) with an initial denaturation at 95°C for 5 min, followed by 40-60 cycles of PCR at 95°C for 5 sec and 50°C for 30 sec, before melting at 95°C for 5 sec and 60°C for 1 min.

The relative difference in expression levels for pri-miR-124-1/-2/-3 in the sorted cells was calculated and presented as described above but with normalization to the control GAPDH.

## **2.8 Luciferase activity assay**

The predicted target genes of miR-124 were identified using a public database (miRWalk2.0, <http://www.umm.uni-heidelberg.de/apps/zmf/mirwalk>). Sections containing the miR-124 binding site of the 3'UTR of Tcf4(v2) and Zbtb46 were cloned into pmirGLO vectors, independently.  $2.5 \times 10^4$  HeLa cells were seeded in a 24-well plate. After 48 hrs, the pmirGLO vector containing the target mRNA binding site for the miR was co-transfected with mmu-miR-124 mimic (TaqMan®) or the negative control using Lipofectamine 2000 (Invitrogen Co, Carlsbad, CA). Luciferase activity was measured after 48 hrs using Dual Luciferase Assay (Promega Corporation, Fitchburg, WI) according to the manufacturer's instructions on a luminometer (Promega). *Renilla* luciferase was used to normalize the transfection efficiency. Each assay was repeated at least 3 times.

## **2.9 miR-124 mimic/inhibitor transfection**

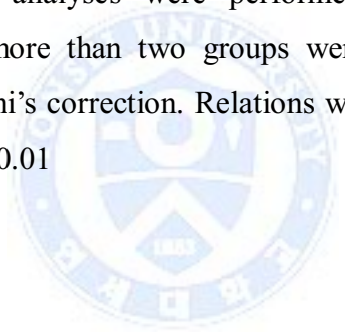
miRCURY Locked Nucleic Acid (LNA) microRNA Mimic (hsa-miR-124-3p), miRCURY LNA Mimic Control (cel-miR-39-3p), miRCURY LNA Power Inhibitor (mmu-miR-124-3p), and miRCURY LNA Power Inhibitor Control from Exiqon (Cambridge, MA) were used at 100 uM. CDPs were transfected with oligonucleotides by nucleofection using Amaxa® P4 Primary Cell 4D-Nucleofector® X Kit (Lonza, Cologne, Germany) reagents and the 4D-Nucleofector® X Unit (Lonza) according to the manufacturer's instructions.

## **2.10 Culture of CDPs and miR-124 transfection**

CDPs were sorted from fresh BM of CD45.2 mice. After nucleofection with the appropriate miR-124 mimic, inhibitor, or control oligonucleotides  $5 \times 10^3$  to  $1.5 \times 10^4$  sorted CDPs were co-cultured with  $5 \times 10^6$  BM cells from CD45.1 mice in 6-well plates using 25% Flt3L-conditioned media. Flow cytometry was used to assess the growth pattern of the CDP populations on day 2 and 4 post-seeding.

## **2.11 Statistical analysis**

The results are expressed as the mean  $\pm$  SD from at least three independent experiments. Statistical analyses were performed using Student's t-test. Comparisons between more than two groups were performed by one-way ANOVA using Bonferroni's correction. Relations were considered statistically significant when the  $p < 0.01$



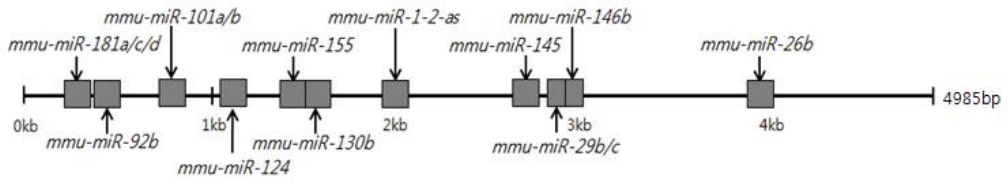
### III. Results

#### 3.1 Candidate miRNAs related to DC development

To identify miRNAs possibly involved in DC development, an online miRNA prediction software (miRWalk2.0) which amalgamates data from a collection of miRNA-target prediction programs was used. Ten gene targets that are prominently known to have a pivotal role in DC development – Tcf4, Bcl6, Irf2, Irf4, Irf8, Id2, SpiB, Batf3, Notch2, Zbtb46 – were picked for the prediction software to identify miRNAs that possibly regulate these genes by binding to their 3'UTR. From the provided candidate list of miRNAs that have a high potential to bind to these transcription factors, candidates with primers that were accessible in an in-house library probe collection, provided in courtesy of Professor Ki-Chul Hwang, were picked out. **Figure 4** shows the 3'UTR map diagram of the 10 transcription factors and the binding sites of the candidate miRNAs. Overall, 20 candidate miRNAs were specified. This allowed identification of miRNAs that potentially bind to the 3'UTR of these essential transcription factors, regulate their activity, and affect DC development.

A

Mouse **Tcf4** 3'UTR

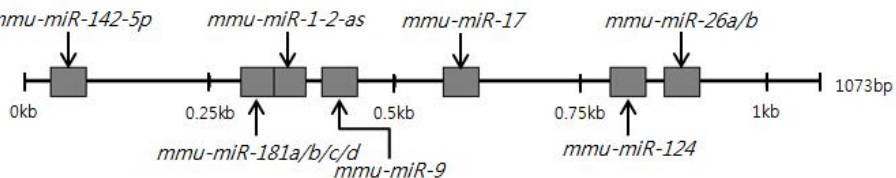


Gene	MicroRNA	StemLoop ID	Sequence (5' → 3')	miRDB	miRWalk	miRanda	Targetscan	SUM
Tcf4	mmu-miR-155	mmu-mir-155	UUAAGUCUAAUUGUAUAGGGGU	1	1	1	1	4
Tcf4	mmu-miR-29b	mmu-mir-29b-2	CUGGUUUCACAUUGGUGGUAGAUU	0	1	1	1	3
Tcf4	mmu-miR-101a	mmu-mir-101a	UACAGUACUGUGAUAAACUGAA	0	1	1	1	3
Tcf4	mmu-miR-26b	mmu-mir-26b	UUCAAGUAAUUCAGGAUAGGU	0	1	1	1	3
Tcf4	mmu-miR-181d	mmu-mir-181d	AACAUUCAUUGUUGCGGUGGGU	0	1	1	1	3
Tcf4	mmu-miR-130b	mmu-mir-130b	CAGUGCAAUGAAGAGGCAU	0	1	1	1	3
Tcf4	mmu-miR-181c	mmu-mir-181c	AACAUUCAACUGUCGUGAGU	0	1	1	1	3
Tcf4	mmu-miR-29c	mmu-mir-29c	UAGCACCAUUGAAUUCGGUUA	0	1	1	1	3
Tcf4	mmu-miR-181a	mmu-mir-181a-1	AACAUUCAACGUGUCGUGAGU	0	1	1	1	3
Tcf4	mmu-miR-124	mmu-mir-124-2	UAAGGCACGCGUGAAUGCC	0	1	1	1	3
Tcf4	mmu-miR-92b	mmu-mir-92b	UAUUGCACUCGUGCCGCCUCC	0	1	1	1	3
Tcf4	mmu-miR-145	mmu-mir-145	GUCCAGUUUCCAGGAUCCCU	0	1	1	1	3
Tcf4	mmu-miR-1-2-as	mmu-mir-1-2-as	UACAUAUUUUUUAACAUCCA	0	1	1	1	3
Tcf4	mmu-miR-101b	mmu-mir-101b	GUACAGUACUGUAUAGCU	0	1	1	1	3
Tcf4	mmu-miR-146b	mmu-mir-146b	UGAGAACUGAAUCCAAGGCU	0	1	1	1	3

*PITA* and *RNA22* omitted because *Tcf4*(v2) not registered.  
Only binding sites of miRNA with SUM ≥ 3 shown.

B

Mouse **Bcl6** 3'UTR



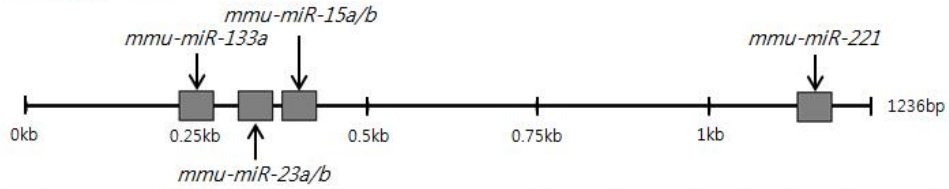
Gene	MicroRNA	StemLoop ID	Sequence (5' → 3')	miRanda	miRDB	miRWalk	PITA	RNA22	Targetscan	SUM
Bcl6	mmu-miR-9	mmu-mir-9-1	UCUUUGGUUAUCUAGCUGUAUGA	1	1	1	1	1	1	6
Bcl6	mmu-miR-17	mmu-mir-17	CAAAGUGCUUACAGUCAGGUAG	0	0	1	1	1	1	4
Bcl6	mmu-miR-181a	mmu-mir-181a-1	AACAUUCAACGUGUCGUGAGU	0	0	1	1	1	1	4
Bcl6	mmu-miR-181b	mmu-mir-181b-1	AACAUUCAUUGCUGUCGUGGGU	0	0	1	1	1	1	4
Bcl6	mmu-miR-181c	mmu-mir-181c	AACAUUCAACGUGUCGUGAGU	0	0	1	1	1	1	4
Bcl6	mmu-miR-181d	mmu-mir-181d	AACAUUCAUUGUUGCGGUGGGU	0	0	1	1	1	1	4
Bcl6	mmu-miR-26a	mmu-mir-26a-1	UUCAAGUAAUCCAGGAUAGGCU	0	0	1	1	1	1	4
Bcl6	mmu-miR-124	mmu-mir-124-1	UAAGGCACGCGUGAAUGCC	1	0	1	1	0	1	4
Bcl6	mmu-miR-142-5p	mmu-mir-142	CAUAAAGUAGAAACACUACU	1	0	1	1	0	1	4
Bcl6	mmu-miR-1-2-as	mmu-mir-1-2-as	UACAUAUUUUUUAACAUCCA	0	0	1	1	0	1	3
Bcl6	mmu-miR-26b	mmu-mir-26b	UUCAAGUAAUUCAGGAUAGGU	0	0	1	1	0	1	3

Only binding sites of miRNA with SUM ≥ 3 shown.



C

Mouse *Irf2* 3'UTR

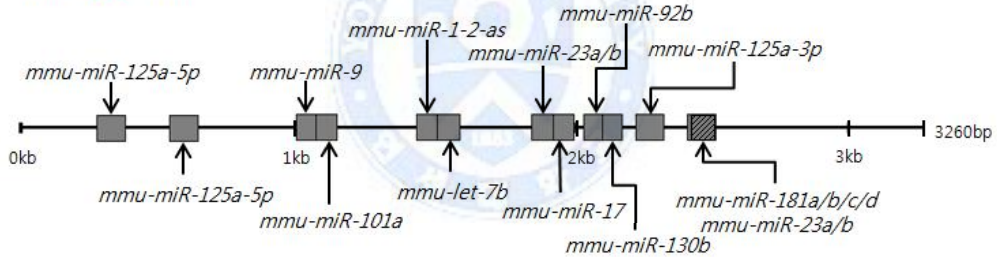


Gene	MicroRNA	StemLoop ID	Sequence (5' → 3')	miRWalk	miRanda	miRDB	PITA	RNA22	Targetscan	SUM
Irf2	mmu-miR-23a	mmu-mir-23a	AUCACAUUGCCAGGGAAUUC	1	1	1	1	0	1	5
Irf2	mmu-miR-23b	mmu-mir-23b	AUCACAUUGCCAGGGAAUAC	1	1	1	1	0	1	5
Irf2	mmu-miR-221	mmu-mir-221	AGCUACAUUGUCUGGGUUUC	1	1	1	1	0	1	5
Irf2	mmu-miR-133a	mmu-mir-133a-2	UUUGGUCCCCUACAACAGCUG	1	1	0	1	0	1	4
Irf2	mmu-miR-15a	mmu-mir-15a	UAGCAGCACAUAAUGUUUGUG	1	0	0	1	1	0	3
Irf2	mmu-miR-15b	mmu-mir-15b	UAGCAGCACAUCAUGUUUACA	1	0	0	1	1	0	3

Only binding sites of miRNA with SUM ≥ 3 shown

D

Mouse *Irf4* 3'UTR



Gene	MicroRNA	StemLoop ID	Sequence (5' → 3')	miRWalk	miRanda	miRDB	PITA	RNA22	Targetscan	SUM
Irf4	mmu-miR-125a-5p	mmu-mir-125a	UCCUGAGACCCUUUAACUGUGA	1	1	1	1	1	1	6
Irf4	mmu-miR-181c	mmu-mir-181c	AACAUAACACUGUCGGUGAGU	1	1	0	1	1	1	5
Irf4	mmu-miR-1-2-as	mmu-mir-1-2-as	UACAUAUCUUUACAUCUCCA	1	1	1	0	1	1	5
Irf4	mmu-miR-181d	mmu-mir-181d	AACAUAUCUUUUGUCGGUGGU	1	1	0	1	1	1	5
Irf4	mmu-miR-23a	mmu-mir-23a	AUCACAUUGCCAGGGAAUUC	1	1	0	1	1	1	5
Irf4	mmu-miR-92b	mmu-mir-92b	UAUUGCACUCGUCGCCGUCC	1	1	0	1	1	1	5
Irf4	mmu-miR-23b	mmu-mir-23b	AUCACAUUGCCAGGGAAUAC	1	1	0	1	1	1	5
Irf4	mmu-miR-181a	mmu-mir-181a-1	AACAUAACACGUCGUGUGAGU	1	1	0	1	1	1	5
Irf4	mmu-miR-130b	mmu-mir-130b	CAGUGCAAUGAUGAAGGGCAU	1	1	0	1	1	1	5
Irf4	mmu-miR-181b	mmu-mir-181b-1	AACAUAUCUUUGUCGGUGGU	1	1	0	1	1	1	5
Irf4	mmu-miR-17	mmu-mir-17	CAAGUGCUUACAGUCAGGUAG	1	0	0	1	1	1	4
Irf4	mmu-miR-101a	mmu-mir-101a	UACAGUACUGUAUACUGAA	1	1	0	0	1	1	4
Irf4	mmu-let-7b	mmu-let-7b	UGAGGUAGUAGGUUGUGUGUU	1	0	0	1	1	1	4
Irf4	mmu-miR-9	mmu-mir-9-1	UCUUUGGUUAUCUAGCUGAUGA	1	0	0	1	1	1	4
Irf4	mmu-miR-146a	mmu-mir-146a	UGAGAACUGAAUCCAUGGGUU	1	0	0	1	1	0	3
Irf4	mmu-miR-125a-3p	mmu-mir-125a	ACAGGUGAGGUUCUUGGGAGCC	0	0	0	1	1	1	3
Irf4	mmu-miR-146b	mmu-mir-146b	UGAGAACUGAAUCCAUGGCU	1	0	0	1	1	0	3

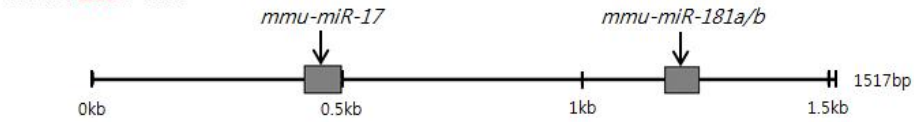
Only binding sites of miRNA with SUM ≥ 3 shown.

Shaded area indicates overlapping binding sites of two distinct microRNAs



**E**

**Mouse *Irf8* 3'UTR**



Gene	MicroRNA	StemLoop ID	Sequence (5' → 3')	miRWalk	miRanda	miRDB	PITA	RNA22	Targetscan	SUM
<i>Irf8</i>	mmu-miR-17	mmu-mir-17	CAAAGUGCUUACAGUCGAGGAG	1	1	0	0	1	1	4
<i>Irf8</i>	mmu-miR-181b	mmu-mir-181b-2	AACAUUCAUUGUCUGCGGUGGU	1	1	0	0	1	1	4
<i>Irf8</i>	mmu-miR-181a	mmu-mir-181a-1	AACAUUCAACGUCUGCGGUGAGU	1	1	0	0	0	1	3

Only binding sites of miRNA with SUM ≥ 3 shown

**F**

**Mouse *Id2* 3'UTR**

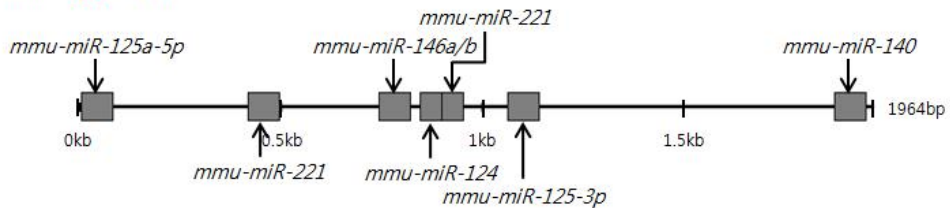


Gene	MicroRNA	StemLoop ID	Sequence (5' → 3')	miRWalk	miRanda	miRDB	PITA	RNA22	Targetscan	SUM
<i>Id2</i>	mmu-miR-181a	mmu-mir-181a-1	AACAUUCAACGUCUGCGGUGAGU	1	1	0	1	1	1	5
<i>Id2</i>	mmu-miR-181d	mmu-mir-181d	AACAUUCAUUGUCUGCGGUGGU	1	1	0	1	1	1	5
<i>Id2</i>	mmu-miR-181b	mmu-mir-181b-2	AACAUUCAUUGUCUGCGGUGGU	1	1	0	1	0	1	4
<i>Id2</i>	mmu-miR-181c	mmu-mir-181c	AACAUUCAACGUCUGCGGUGAGU	1	1	1	0	0	1	4
<i>Id2</i>	mmu-miR-142-5p	mmu-mir-142	CAUAAAGUAGAAAGCACUACU	0	0	0	1	1	1	3
<i>Id2</i>	mmu-miR-155	mmu-mir-155	UUAUAGCUAAUUGUGAUAGGGGU	1	0	0	1	0	1	3

Only binding sites of miRNA with SUM ≥ 3 shown

**G**

**Mouse *Spib* 3'UTR**

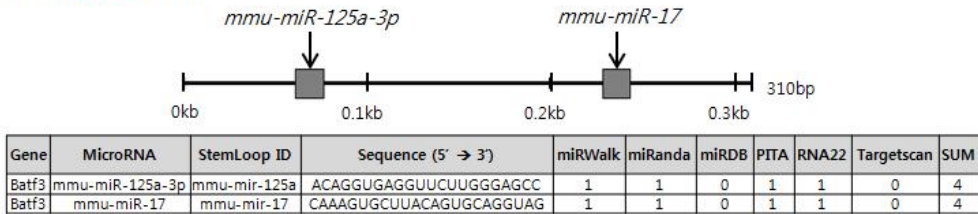


Gene	MicroRNA	StemLoop ID	Sequence (5' → 3')	miRWalk	miRanda	miRDB	PITA	RNA22	Targetscan	SUM
<i>Spib</i>	mmu-miR-221	mmu-mir-221	AGCUACAUUGUCUGCGGUGUUC	1	1	0	1	1	1	5
<i>Spib</i>	mmu-miR-146b	mmu-mir-146b	UGAGAACUGAAUCCAUAGGCU	1	1	0	1	0	1	4
<i>Spib</i>	mmu-miR-146a	mmu-mir-146a	UGAGAACUGAAUCCAUAGGCU	1	1	0	1	0	1	4
<i>Spib</i>	mmu-miR-124	mmu-mir-124-2	UAAGGCACGCGUGAAUGCC	1	1	0	1	0	1	4
<i>Spib</i>	mmu-miR-140	mmu-mir-140	CAGUGGUUUUACCCUUAUGGUAG	0	0	0	1	1	1	3
<i>Spib</i>	mmu-miR-125a-3p	mmu-mir-125a	ACAGGUGAGGUUCUUGGAGCC	1	0	0	1	1	0	3
<i>Spib</i>	mmu-miR-125a-5p	mmu-mir-125a	UCCUGAGACCCUUUAACCGUGA	1	0	0	1	1	0	3

Only binding sites of miRNA with SUM ≥ 3 shown

## H

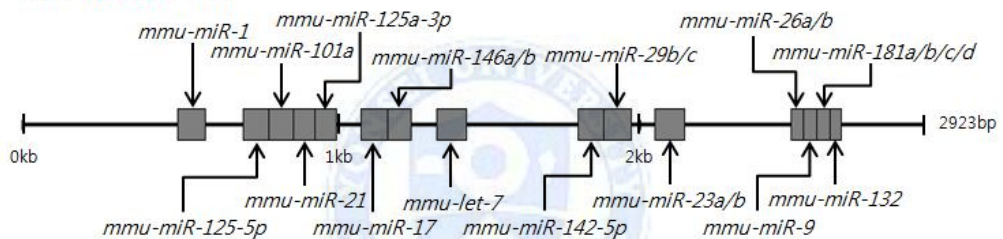
### Mouse **Batf3** 3'UTR



Only binding sites of miRNA with SUM ≥ 3 shown

## I

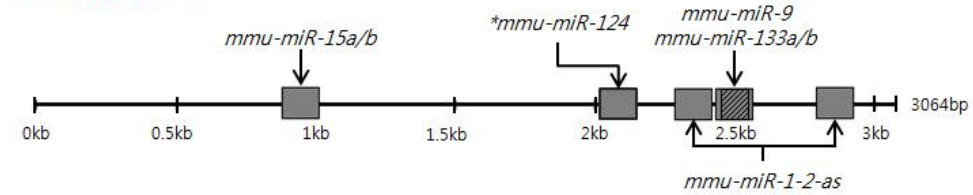
### Mouse **Notch2** 3'UTR



Gene	MicroRNA	StemLoop ID	Sequence (5' → 3')	miRWalk	miRanda	miRDB	PITA	RNA22	Target scan	SUM
Notch2	mmu-miR-9	mmu-mir-9-1	UCUUUGGUUAUCUAGCUGUAUGA	1	1	1	1	1	1	6
Notch2	mmu-miR-181c	mmu-mir-181c	AACAUUCAACCGUCGUGAGU	1	1	0	1	1	1	5
Notch2	mmu-miR-181a	mmu-mir-181a-1	AACAUUCAACCGUCGUGAGU	1	1	0	1	1	1	5
Notch2	mmu-miR-21	mmu-mir-21a	UAGCUUAUCAGACUGAUGUUA	1	1	0	1	1	1	5
Notch2	mmu-miR-142-5p	mmu-mir-142	CAUAAAGUAGAAAGCACUACU	1	1	0	1	1	1	5
Notch2	mmu-miR-125a-3p	mmu-mir-125a	ACAGGUGAGGUUCUUGGGAGCC	1	1	0	1	1	1	5
Notch2	mmu-let-7e	mmu-mir-7e	UGAGGUAGGAGGUUGUAUAGUU	1	0	0	1	1	1	4
Notch2	mmu-miR-101a	mmu-mir-101a	UACAGUACUGUAUACUGAA	1	1	0	1	0	1	4
Notch2	mmu-let-7a	mmu-mir-7a-1	UGAGGUAGUAGGUUGUAUAGUU	1	0	0	1	1	1	4
Notch2	mmu-miR-132	mmu-mir-132	UACAGUACUACGCCAUGGUGC	1	1	0	1	0	1	4
Notch2	mmu-let-7f	mmu-mir-7f-1	UGAGGUAGUAGAUUGUAUAGUU	1	0	0	1	1	1	4
Notch2	mmu-miR-1	mmu-mir-1a-1	UGGAAUGUAAAGAAUGUAU	1	1	0	1	0	1	4
Notch2	mmu-let-7b	mmu-mir-7b	UGAGGUAGUAGGUUGUGUGGUU	1	0	0	1	1	1	4
Notch2	mmu-miR-26a	mmu-mir-26a-1	UUCAAGUAAUCCAGGAUAGGU	1	0	0	1	1	1	4
Notch2	mmu-let-7g	mmu-mir-7g	UGAGGUAGUAGUUUGUACAGUU	1	0	0	1	1	1	4
Notch2	mmu-miR-146a	mmu-mir-146a	UGAGAACUGAAUCCAUUGGGUU	1	0	0	1	1	1	4
Notch2	mmu-let-7c	mmu-mir-7c	UGAGGUAGUAGGUUGUAUAGUU	1	0	0	1	1	1	4
Notch2	mmu-miR-181b	mmu-mir-181b-1	AACAUUCAUUGCUGUCGUGGGU	0	1	0	1	1	1	4
Notch2	mmu-let-7i	mmu-mir-7i	UGAGGUAGUAGUUUGUGCUGUU	1	0	0	1	1	1	4
Notch2	mmu-let-7d	mmu-mir-7d	CUAUACGACCGUCGCCUUUCU	0	0	0	1	1	1	3
Notch2	mmu-miR-181d	mmu-mir-181d	AACAUUCAUUGUUGCGUGGGU	0	1	0	1	0	1	3
Notch2	mmu-miR-17	mmu-mir-17	CAAAGUGCUUACAGUGCAGGUAG	1	0	0	1	1	0	3
Notch2	mmu-miR-23a	mmu-mir-23a	AUCACAUUGCCAGGGAUUAUCC	0	0	0	1	1	1	3
Notch2	mmu-miR-29b	mmu-mir-29b-2	CUGGUUUACAUUGGUGCUUAGAUU	1	0	0	1	1	0	3
Notch2	mmu-miR-23b	mmu-mir-23b	AUCACAUUGCCAGGGAUUAUCC	0	0	0	1	1	1	3
Notch2	mmu-miR-26b	mmu-mir-26b	UUCAAGUAAUCCAGGAUAGGU	1	0	0	1	0	1	3
Notch2	mmu-miR-29c	mmu-mir-29c	UAGCACC AUUUGAAUUCGUAU	1	0	0	1	1	0	3
Notch2	mmu-miR-146b	mmu-mir-146b	UGAGAACUGAAUCCAUAGGU	1	0	0	1	0	1	3
Notch2	mmu-miR-125a-5p	mmu-mir-125a	UCCUGAGACCCUUUAACUGUGA	1	0	0	1	1	0	3

Only binding sites of miRNA with SUM ≥ 3 shown

J

Mouse **Zbtb46** 3'UTR

Gene	MicroRNA	StemLoop ID	Sequence (5' → 3')	miRWalk	miRanda	miRDB	RNA22	Targetscan	SUM
Zbtb46	mmu-miR-9	mmu-mir-9-1	UCUUUGGUUAUCUAGCUGUAUGA	1	1	0	1	1	4
Zbtb46	mmu-miR-1-2-as	mmu-mir-1-2-as	UACAUACUUCUUUACAUCUCCA	1	1	0	1	1	4
Zbtb46	mmu-miR-133b	mmu-mir-133b	UUUGGUCCCCUUAACACAGCUA	1	0	0	1	1	3
Zbtb46	mmu-miR-15a	mmu-mir-15a	UAGCAGCACAUAAUGGUUUUGUG	1	0	0	1	1	3
Zbtb46	mmu-miR-15b	mmu-mir-15b	UAGCAGCACAUCAUGGUUUUACA	1	0	0	1	1	3
Zbtb46	mmu-miR-133a	mmu-mir-133a-2	UUUGGUCCCCUUAACACAGCUG	1	0	0	1	1	3

*PITA omitted because Zbtb46 not registered*

*Only binding sites of miRNA with SUM ≥ 3 shown*

*Shaded area indicates overlapping binding sites of two distinct microRNAs*

*\*mmu-miR-124 not in chart because SUM < 3*

**Figure 4. Identification of candidate miRNAs that potentially target the transcript of transcription factors in DC development.** miRWalk2.0 was used to identify miRNAs with high probability to bind to the 3'UTR of the listed transcription factors. miRanda, miRWalk, miRDB, PITA, RNA22, and TargetScan prediction algorithms were used and miRNAs with significant scores from at least 3 of the algorithms were listed (SUM ≥ 3). (A) Candidate list of miRNAs that target Tcf4 and the map diagram of Tcf4 3'UTR with the predicted binding sites of the candidates. The same is shown for (B) Bcl6, (C) Irf2, (D) Irf4, (E) Irf8, (F) Id2, (G) SpiB, (H) Batf3, (I) Notch2, and (J) Zbtb46.

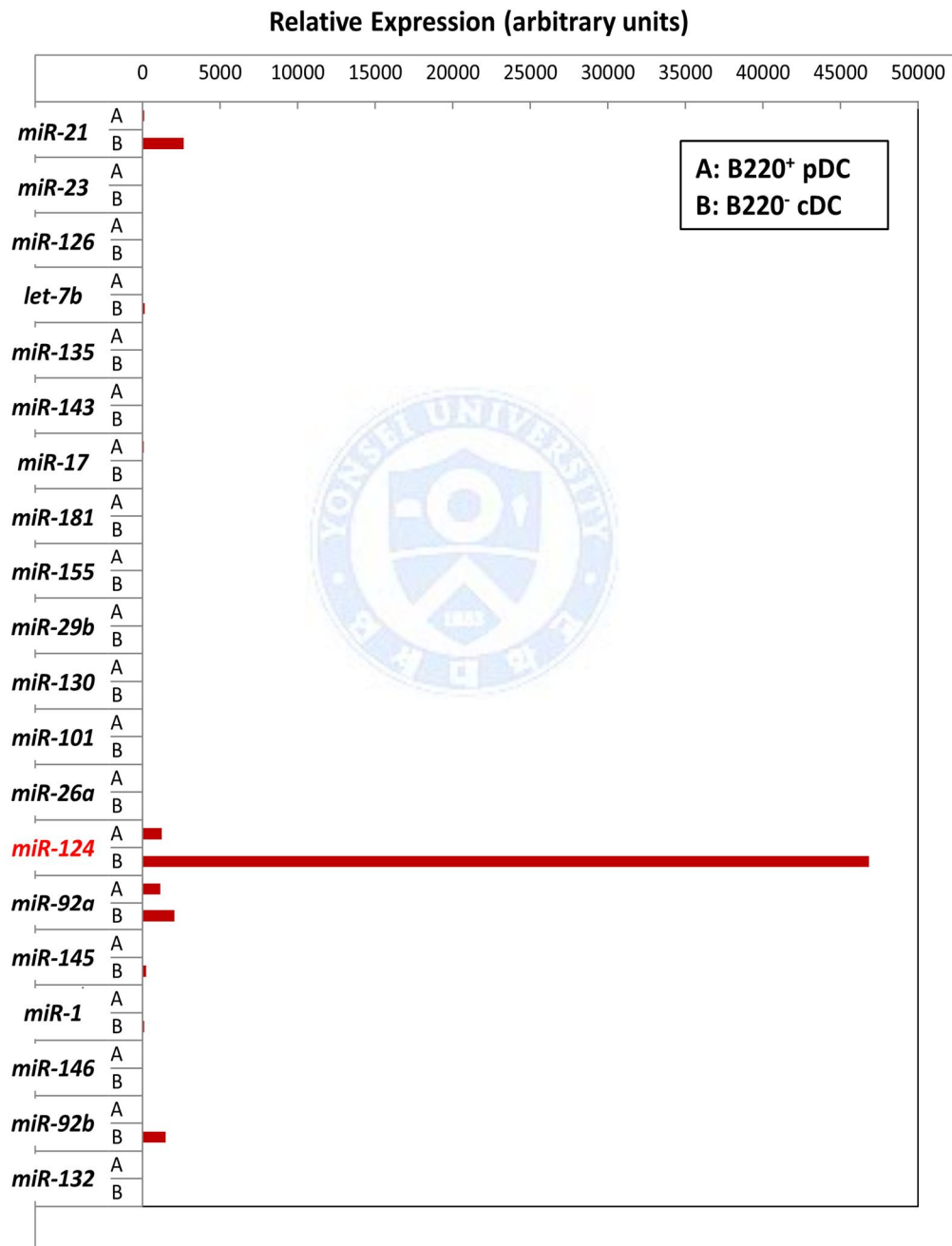
### 3.2 miR-124 is outstandingly expressed in DC subset

In preliminary efforts to identify unmentioned miRNA that may play a role in DC development, expression profiles were observed in both the GM-CSF and Flt3L culture systems of murine BM cells. Initial screenings of miRNAs in the GM-CSF culture system saw a drastic increase in the expression of miR-155 in correlation with the differentiation into MoDCs. This was corroborated in a recent corresponding publication by Reith *et al.* which explained the importance of miR-155 in the silencing of c-Fos expression for the development and functional maturation of MoDCs.<sup>5</sup>

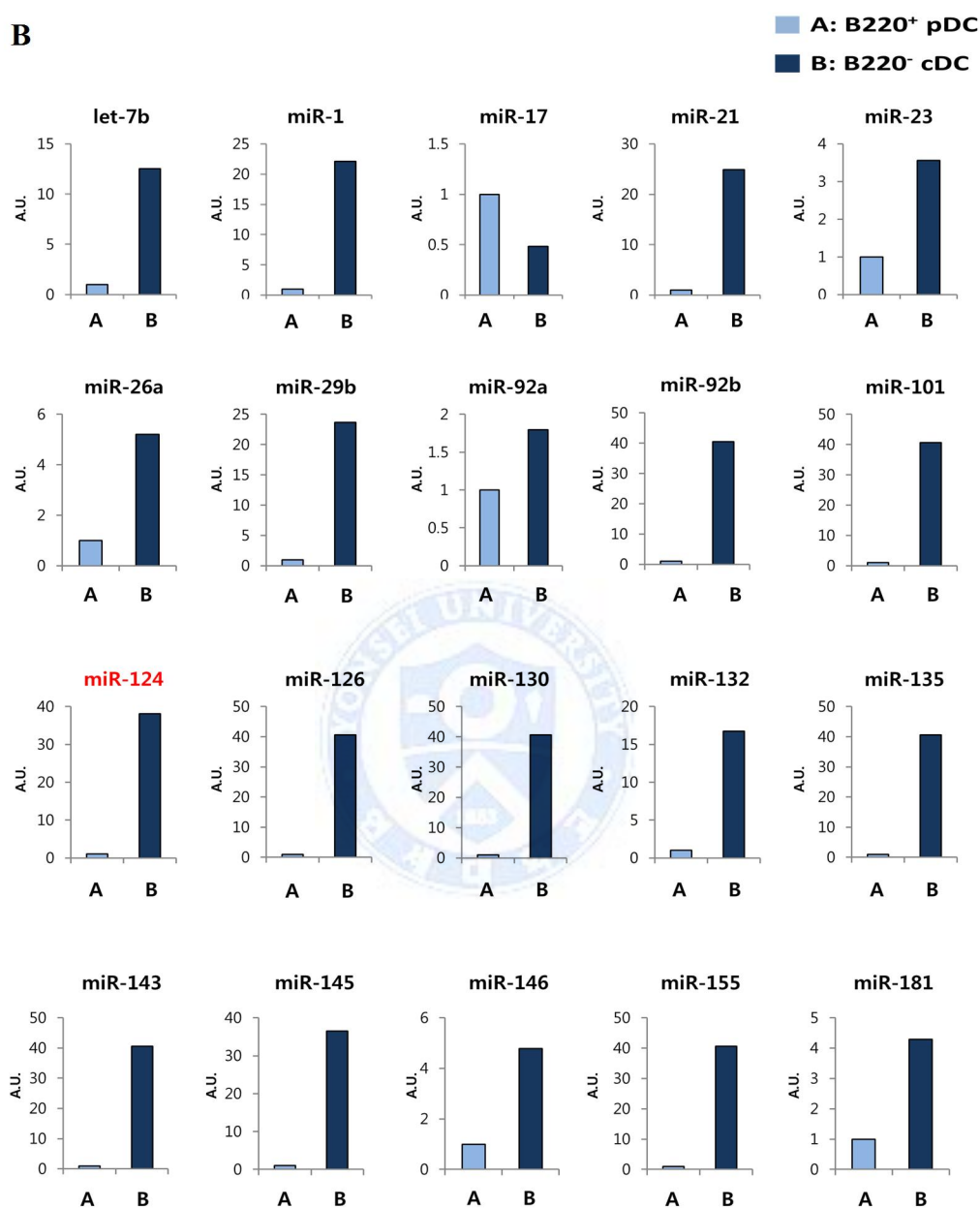
miRNA expression profiles were then observed in the Flt3L culture system. More specifically, for further evidence of miRNAs possibly involved in DC differentiation, the in-house probe collection was used to perform an initial expression screening of the candidate miRNAs in BM B220<sup>-</sup> cDCs and B220<sup>+</sup> pDCs. The RNAs of these two general matureDC subsets generated by Flt3L-conditioned media were isolated and the expression profile of the candidate miRNAs were observed by real-time PCR. Normalization to the lowest expression showed an exceedingly high relative expression of miR-124 in B220<sup>-</sup> cDCs compared to other candidate miRNAs (**Figure 5A**). Normalization to each individual candidate miRNA showed that most miRNAs are expressed more in B220<sup>-</sup> cDCs except for miR-17 (**Figure 5B**). The outstanding expression of miR-124 in B220<sup>-</sup> cDCs and its contrasting expression between the two DC groups hint that miR-124 may be expressed differentially within DC ontogeny and may play a role in their development.

A

## In-house primer library screening of relevant miRNA in dendritic cell (DC) subsets





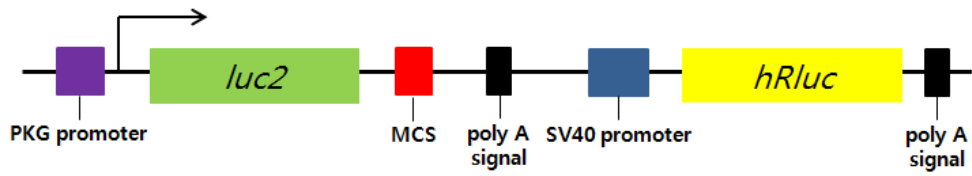
**B**

**Figure 5. Initial expression screening of candidate miRNAs.** (A) Real-time PCR screening showing relative expression levels of candidate miRNAs in BM B220<sup>-</sup> cDCs and B220<sup>+</sup> pDCs. (B) Expression levels of candidate miRNAs normalized to individual candidate miRNA probes.

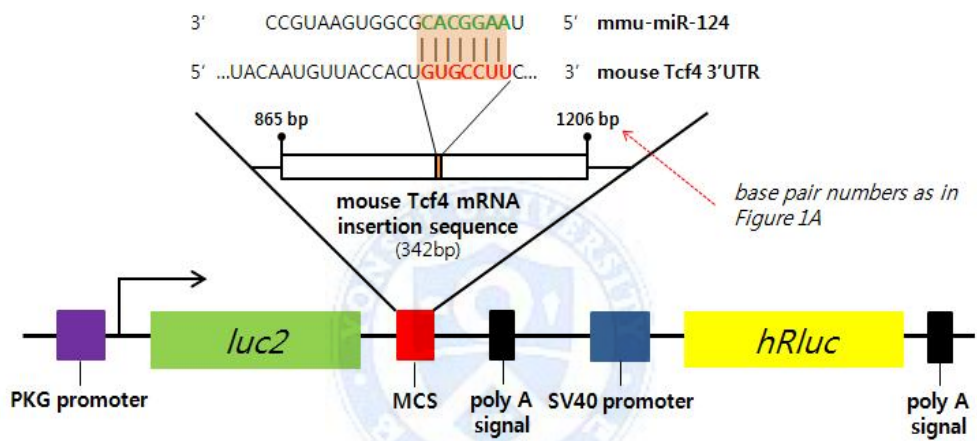
### 3.3 miR-124 might directly regulate Tcf4 activity

In light of the previous data, focus was concentrated on miR-124 to uncover if it may have a role in DC development. The prediction algorithm programs were used to see the possible transcription factor targets of miR-124. miR-124 was shown to have a high probability of binding to the 3'UTR of Tcf4 (**Figure 4A**). miR-124 was also predicted to bind to Zbtb46 (not shown in chart  $\therefore$  SUM < 3). To see whether miR-124 actually binds to these genes, a dual luciferase reporter assay was performed. A section, 342bps, of the 3'UTR of Tcf4 containing the predicted binding site of miR-124 was inserted into the multiple cloning site (MCS) of a pmirGLO vector (**Figure 6A**). A 480bp section of the 3'UTR of Zbtb46 was done the same (**Figure 6B**). The cloned vectors were co-transfected with miR-124 mimic or the negative control into HeLa cells and the luciferase activity was measured. The assay showed that the overexpression of miR-124 caused a decrease in luciferase activity of the pGLO-Tcf4 vector (~30%) while not that of pGLO-Zbtb46 (**Figure 6C**). This indicates that miR-124 directly binds to the 3'UTR of Tcf4 and regulates its activity. Mentioned before, Tcf4 is a critical gene in the development and homeostasis of pDCs.<sup>3</sup> Together these findings suggest that miR-124 may directly regulate Tcf4 activity and play a pivotal role in DC development.

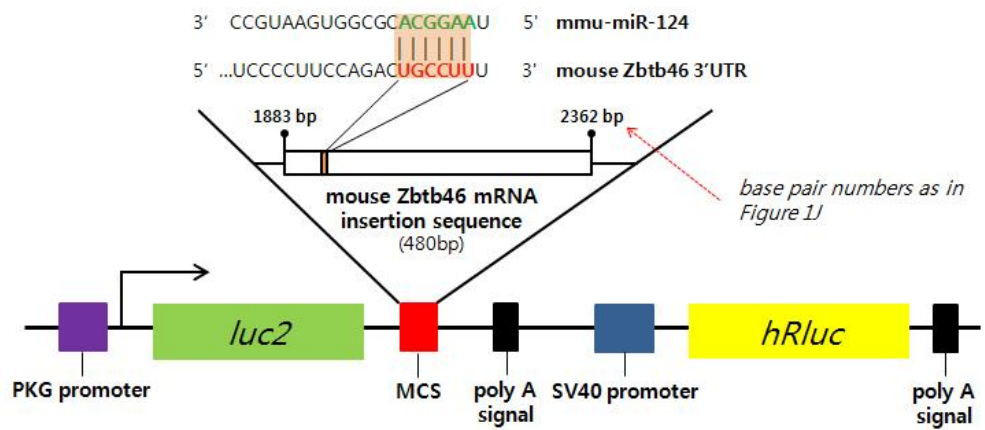
A



B



C





**D**

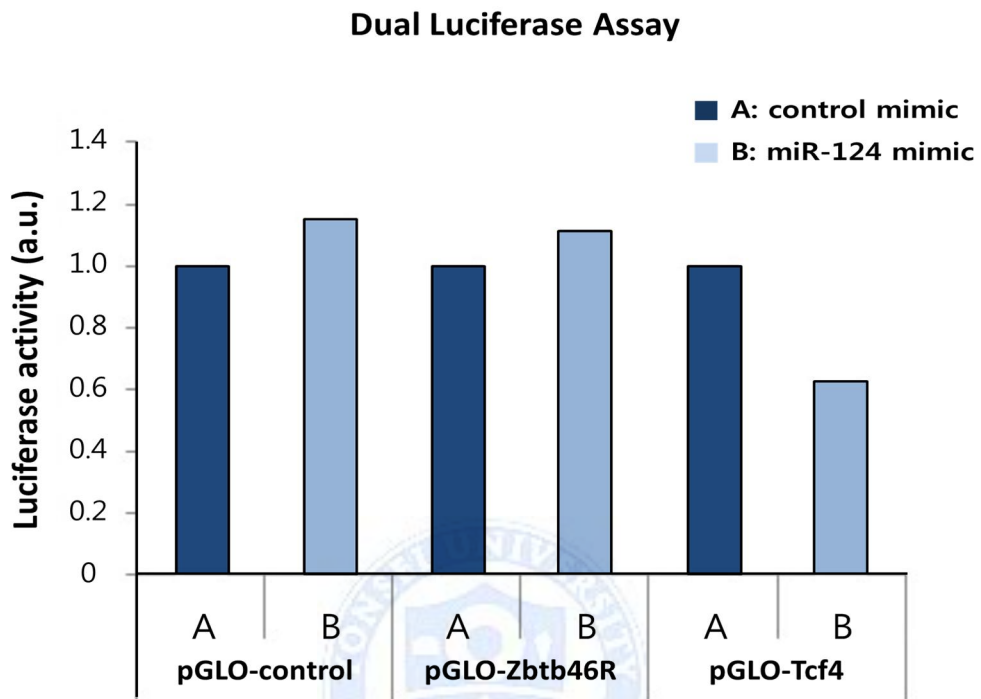
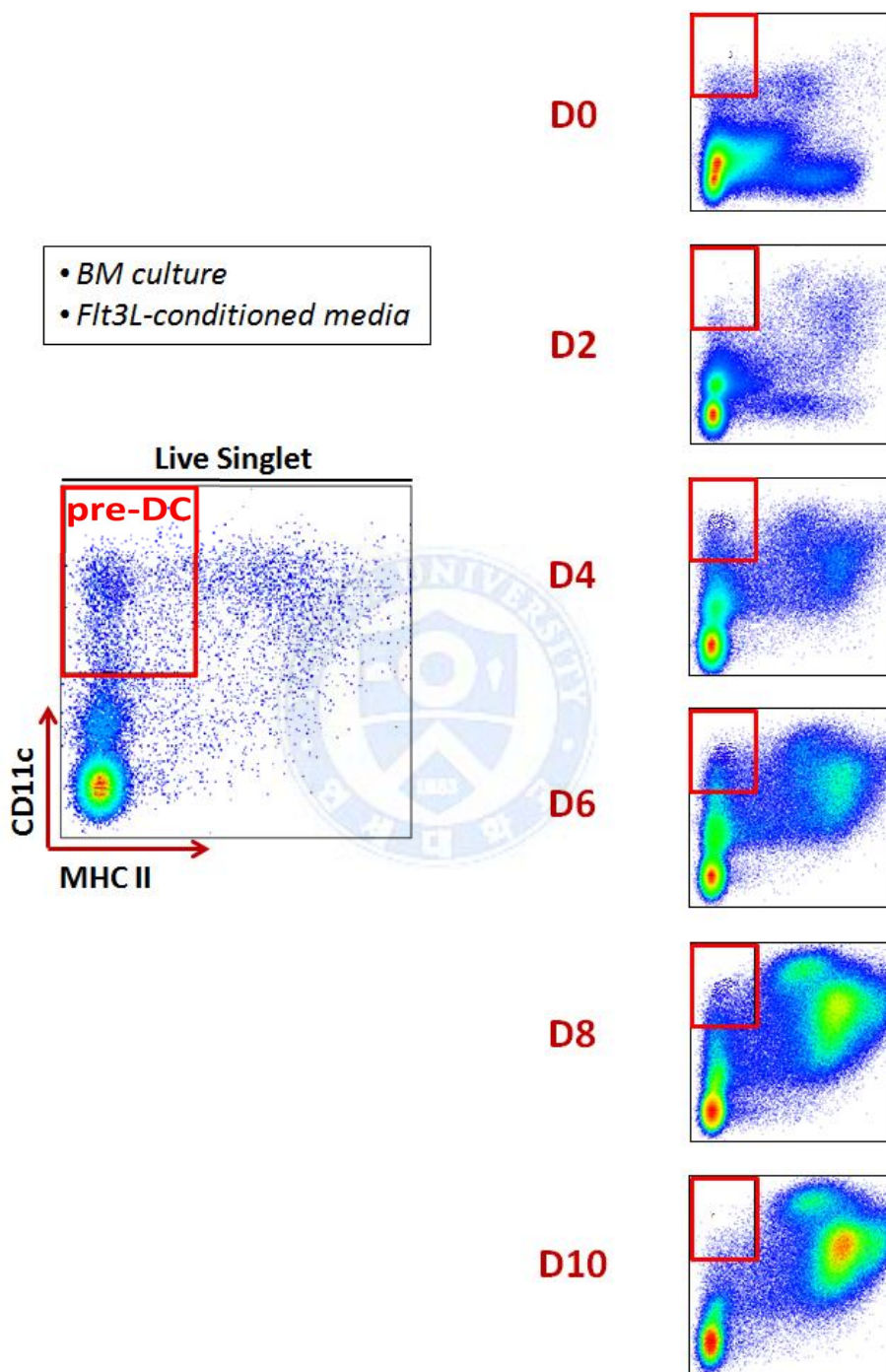


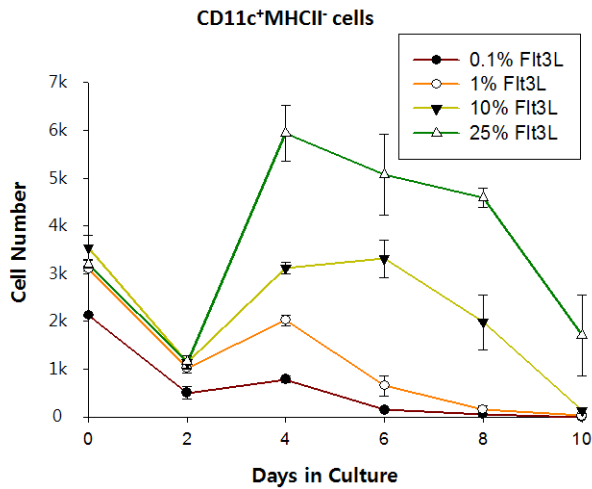
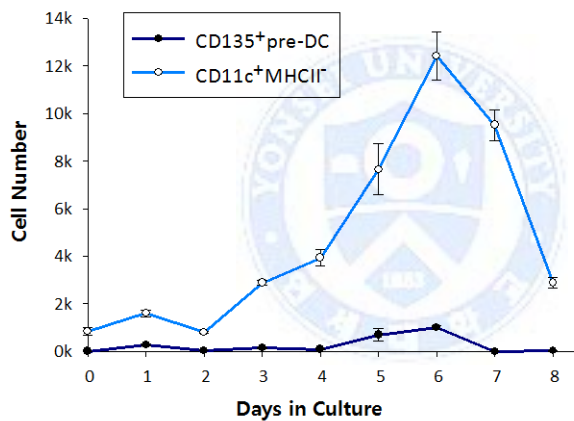
**Figure 6. miR-124 directly regulates the 3'UTR of Tcf4.** (A) pmirGLO vector map diagram. (B) Map diagram of pmirGLO vector with section of Tcf4 3'UTR containing the predicted binding site for miR-124 inserted into the MCS. (C) Map diagram of pmirGLO-Zbtb46 vector. (D) Dual luciferase reporter assay of the clone vectors shows luciferase activity in pGLO-Tcf4 and pGLO-Zbtb46 after treatment with miR-124 mimic or control mimic.

### 3.4 Bone marrow cells differentiate into distinct subsets upon culture with Flt3L

In order to verify the developmental pattern of DC subsets as described in previous publications, time-course analyses of DC development in Flt3L culture was performed.<sup>16</sup> First, to optimize culture conditions, a time-course analysis of DC subsets was performed with serial dilutions of Flt3L. A Flt3L titration culture of murine BM cells was performed and the development of subsets were analyzed by flow cytometry every 2 days for 10 days. The pre-DC subset was broadly gated as CD11c<sup>+</sup>MHCII<sup>-</sup> (**Figure 7A**). pDC population was defined as CD11c<sup>+</sup>B220<sup>+</sup> cells (**Figure 8A**), while cDC1 and cDC2 lineages were defined as CD11c<sup>+</sup>B220<sup>-</sup>CD24<sup>hi</sup>CD172a<sup>-</sup> and CD11c<sup>+</sup>B220<sup>-</sup>CD24<sup>lo</sup>CD172a<sup>+</sup> respectively (**Figure 9A**). The results indicated 25% Flt3L-conditioned media sufficiently provided hospitable environments for pre-DCs (**Figure 7**) or matureDCs to thrive (**Figure 8, 9**). Higher concentrations were able to induce DC differentiation and maturation more efficiently as previously described.<sup>22</sup> The overall BM DC growth patterns in Flt3L-conditioned media were similar to the observations made by Shortman *et al.*<sup>16</sup> and Murphy *et al.*<sup>15</sup> The pre-DC subset showed to initially decrease in number, increase up to 4 to 6 days post-culture, and then steady decline in further culture (**Figure 7B,C**). The pDC population showed to generate abundantly starting from day 4 post-culture, peak at day 6 post-culture, and plateau in number until day 10 post-culture (**Figure 8B**). Meanwhile, both cDC1 and cDC2 lineages showed to steadily increase in number and peak at day 8 post-culture before declining (**Figure 9B**). These data allowed formulation of a proficient system of BM DC subset culture with 25% Flt3L-conditioned media, and provided a guiding frame for further isolation studies.

A



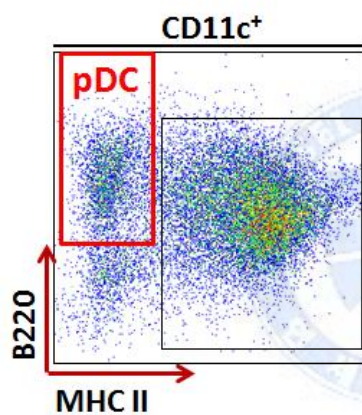
**B****C**

**Figure 7. *In vitro* generation of pre-DCs by culture of BM cells with Flt3L.**

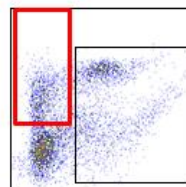
Mouse BM cells were cultured in various concentrations of Flt3L-conditioned media for 10 days. (A) Time-course FACS analysis of CD11c<sup>+</sup>MHCII<sup>-</sup> cells every 2 days for 10 days in culture with 25% Flt3L-conditioned media. BM cells were seeded in 24-well plates at 1x10<sup>6</sup> cells per well. (B) Graphical representation of CD11c<sup>+</sup>MHCII<sup>-</sup> cell number over 10 days of culture in various concentrations of Flt3L. (C) Graphical representation of CD11c<sup>+</sup>MHCII<sup>-</sup> cell number and CD135<sup>+</sup> pre-DC cell number over 8 days in culture with 25% Flt3L-conditioned media.

A

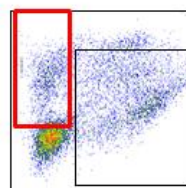
- *BM culture*
- *25% Flt3L-conditioned media*



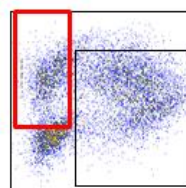
D0



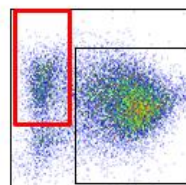
D2



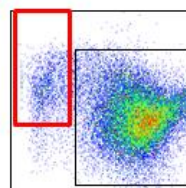
D4



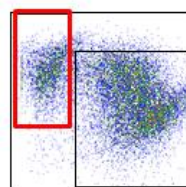
D6



D8



D10



**B**

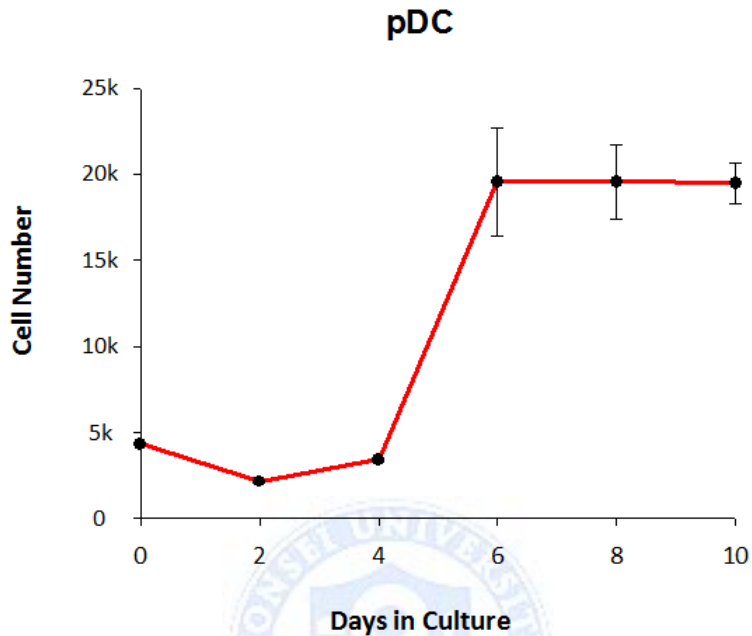
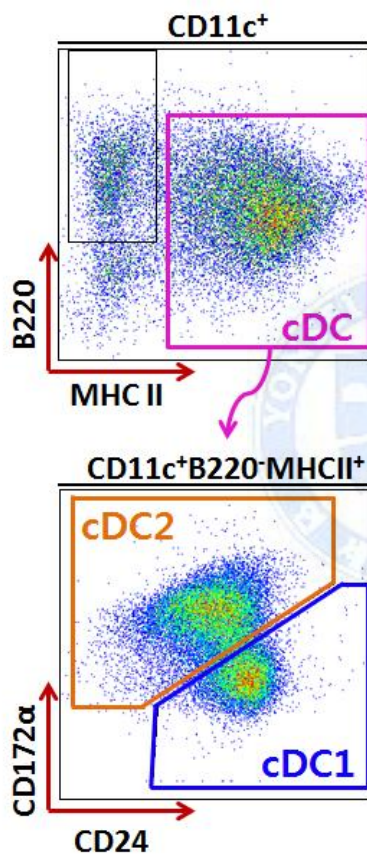


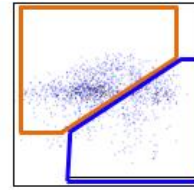
**Figure 8. *In vitro* generation of pDCs by culture of BM cells with Flt3L.** Mouse BM cells were cultured in Flt3L-conditioned media for 10 days. (A) Time-course FACS analysis of pDC population gated as CD11c<sup>+</sup>MHCII<sup>+</sup>B220<sup>+</sup> cells every 2 days for 10 days in 25% Flt3L-conditioned media. BM cells were seeded in 24-well plates at  $1 \times 10^6$  cells per well. (B) Graphical representation of pDC cell number over the 10 days in 25% Flt3L-conditioned media.

A

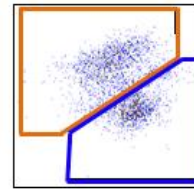
- *BM culture*
- *25% Flt3L-conditioned media*



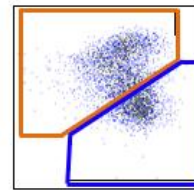
D0



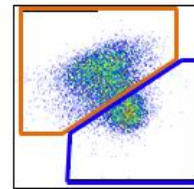
D2



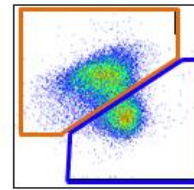
D4



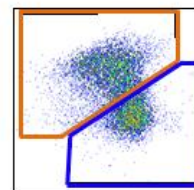
D6



D8



D10



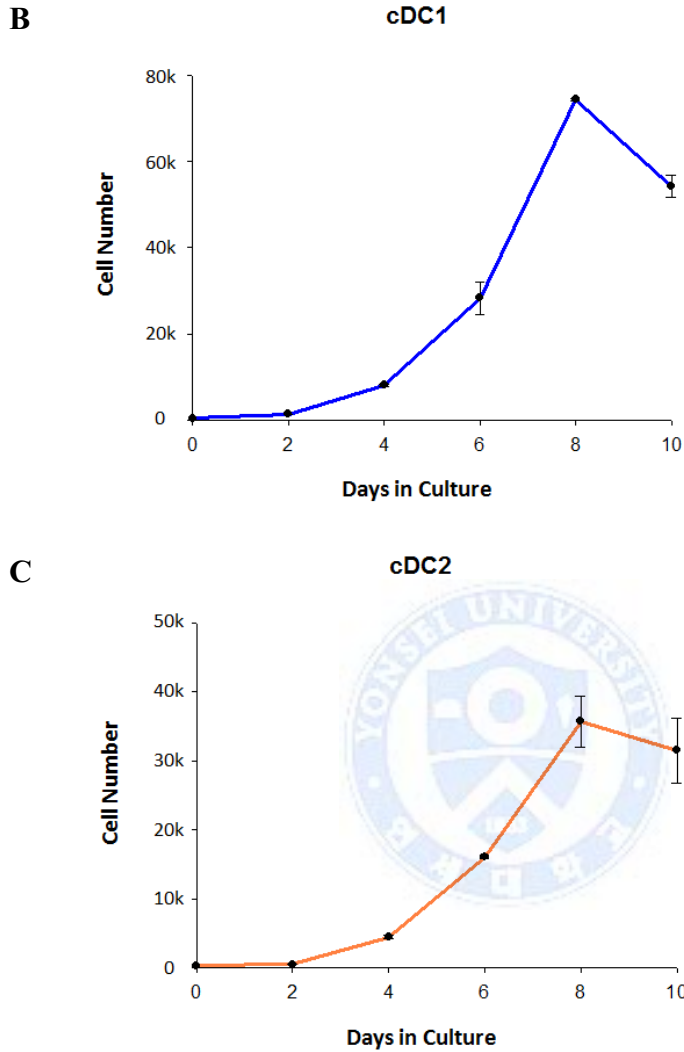


**Figure 9. *In vitro* generation of cDCs by culture of BM cells with Flt3L.** (A) Time-course FACS analysis of cDC1 and cDC2 lineages gated as  $CD11c^{+}MHCII^{+}B220^{-}CD24^{hi}CD172\alpha^{-}$  and  $CD11c^{+}MHCII^{+}B220^{-}CD24^{int}CD172\alpha^{+}$ , respectively, every 2 days for 10 days in 25% Flt3L-conditioned media. BM cells were seeded in 24-well plates at  $1 \times 10^6$  cells per well. (B) Graphical representation of cDC1 cell number and (C) cDC2 cell number over 10 days in 25% Flt3L-conditioned media.



### 3.5 pre-DCs cultured *in vitro* with Flt3L show high expression of miR-124

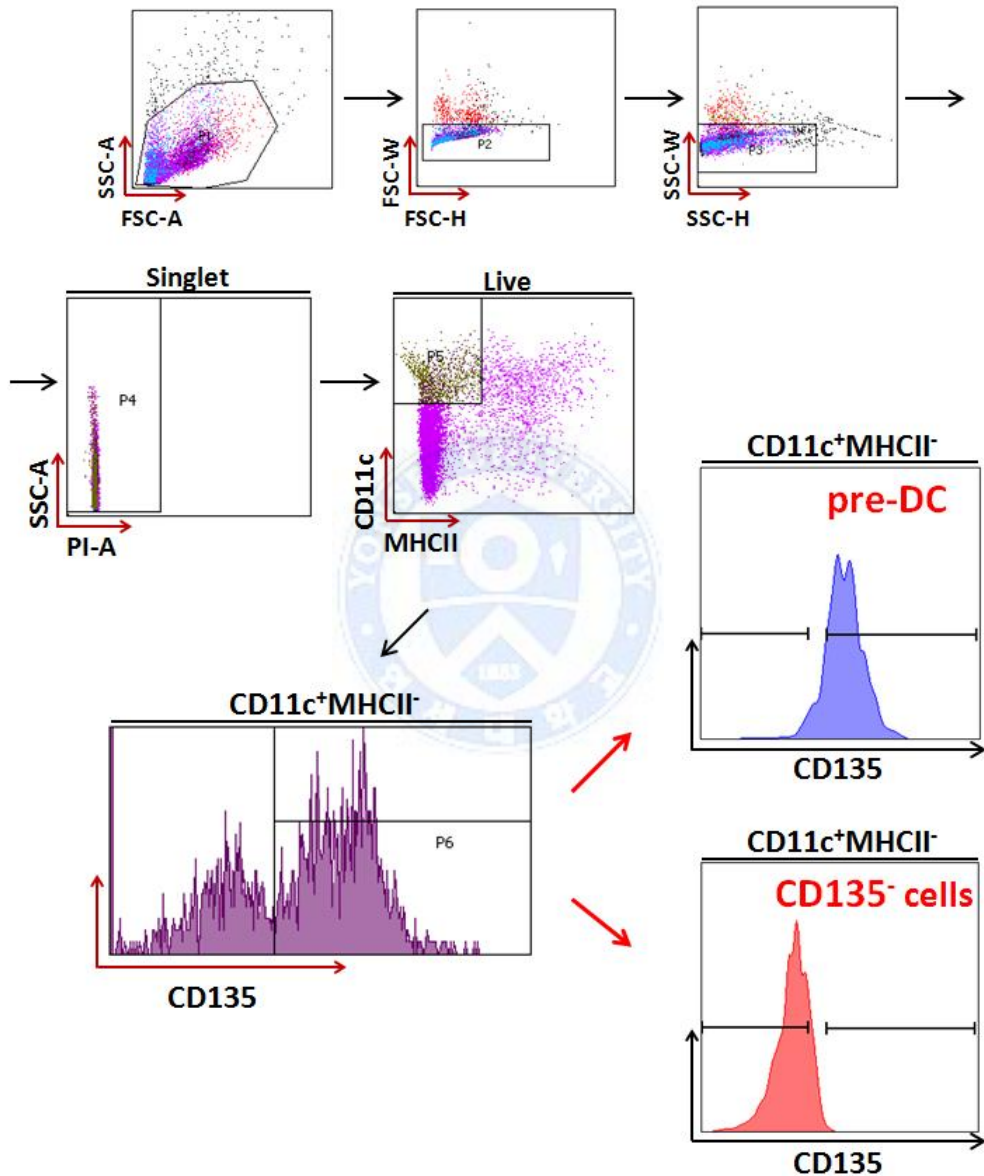
Before examining miRNA levels or any further relevant data, DC subtypes must be successfully isolated from the Flt3L culture system of murine BM cells. In a publication by Shortman *et al.*, the authors demonstrate a high yield isolation of three DC populations through the culture of bone marrow cells with Flt3L for 8 to 10 days. These populations are segregated into CD11c<sup>+</sup>B220<sup>hi</sup> pDCs and CD11c<sup>+</sup>B220<sup>lo</sup> cDCs. The cDC population is shown to be further separated into cDC1 and cDC2 subpopulations using CD24 and CD172 $\alpha$  markers. The authors also demonstrate the efficient isolation of pre-DCs with full capacity to form other hematopoietic lineages and DCs from BM cells after 3.5 days of Flt3L culture. The time frame was determined to offer a high yield of pre-DCs with most irrelevant cells dead and their proliferative potential least diminished.<sup>16</sup> These findings are further corroborated in other publications which demonstrate the isolation of DC subsets by Flt3L culture of murine BM cells and subsequently performing FACS using selected surface markers.<sup>14</sup> Together with the optimized Flt3L culture system delineated in **Figure 7-9**, these guidelines were followed to sort and isolate pre-DC, pDCs, and cDC subsets. After experimentation with a combination of surface markers and strategies, population sorting was optimized to a good yield (purity > 90%). Pre-DCs were isolated by sorting for CD11c<sup>+</sup>MHCII<sup>-</sup>CD135<sup>+</sup> cells after 4 days of 25% Flt3L-conditioned media culture of murine BM cells (**Figure 10A**). MatureDC populations were isolated 10 days after culture of BM cells with 25% Flt3L-conditioned media and sorted as follows: CD11c<sup>+</sup>B220<sup>+</sup> for pDC (**Figure 10B**); CD11c<sup>+</sup>B220<sup>-</sup>CD24<sup>hi</sup>CD172 $\alpha$ <sup>-</sup> for cDC1; and CD11c<sup>+</sup>B220<sup>-</sup>CD24<sup>int</sup>CD172 $\alpha$ <sup>+</sup> for cDC2 (**Figure 10C**).

After successful sorting of the *in vitro*-generated DC subsets, the RNA of the isolated cells were extracted. Real-time PCR of the RNAs with the mmu-miR-124 primer showed an exceedingly high relative expression of miR-124 in pre-DCs compared to the matureDC subsets (**Figure 10D**). The expression of miR-124 in pre-DCs was compared to that of CD11c<sup>+</sup>MHCII<sup>-</sup>CD135<sup>-</sup> negative control cells sorted from the same mice to confirm that the high expression was in fact restricted to the sorted pre-DC population (**Figure 10E**). There was also a repeated pattern of high expression in cDC1 cells among the cultured matureDC subsets (**Figure 10F**).

As mentioned before, the dynamic expression of pivotal transcription factors across DC subsets have been described.<sup>14</sup> Real-time PCR with the probes of selected transcription factors were performed with the RNA of the sorted subsets. The genes observed were: TCF4, IRF8, SFP11, SPIB, STAT3, GFI, BATF3, and ID2. The expression profile of TCF4, BATF3, and IRF8 are shown in **Figure 10G**. The overall patterns of transcription factor expression across the subsets isolated from *in vitro* Flt3L culture were parallel to previously reported patterns indicating genuity of the isolated subsets.<sup>14</sup> TCF4 showed to have high expression in pDCs, while BATF3 and IRF8 showed high expression in cDC1 cells. This correlates with conclusions made by Murphy *et al.*<sup>15</sup>

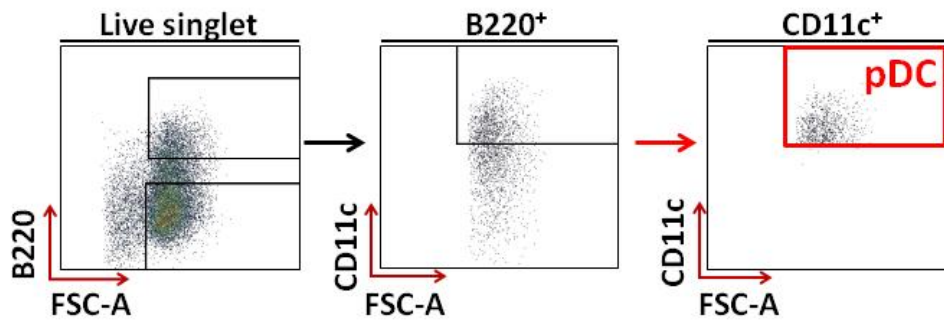
A

# Bone marrow culture day 4 (25% Flt3L-conditioned media)



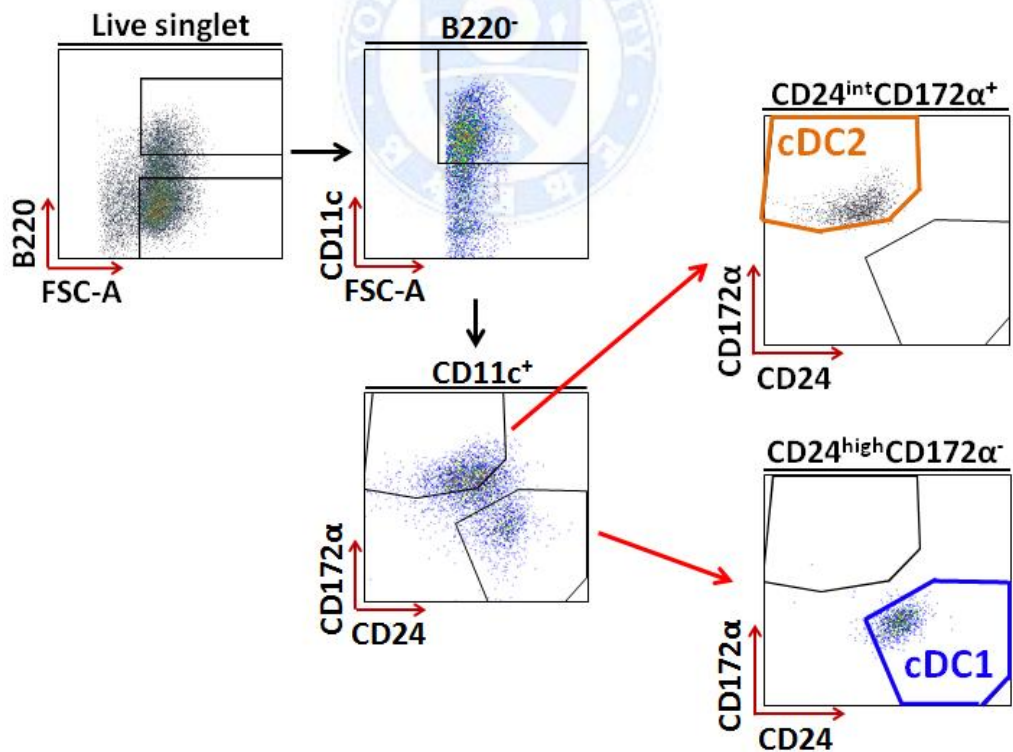
B

Bone marrow culture day 10 (25% Flt3L-conditioned media)

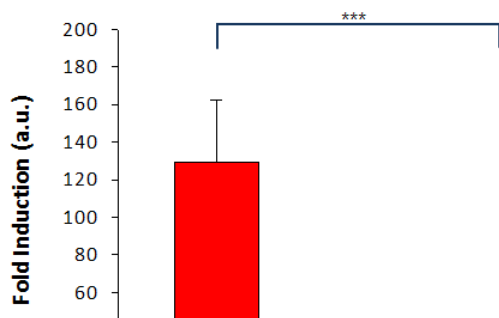


C

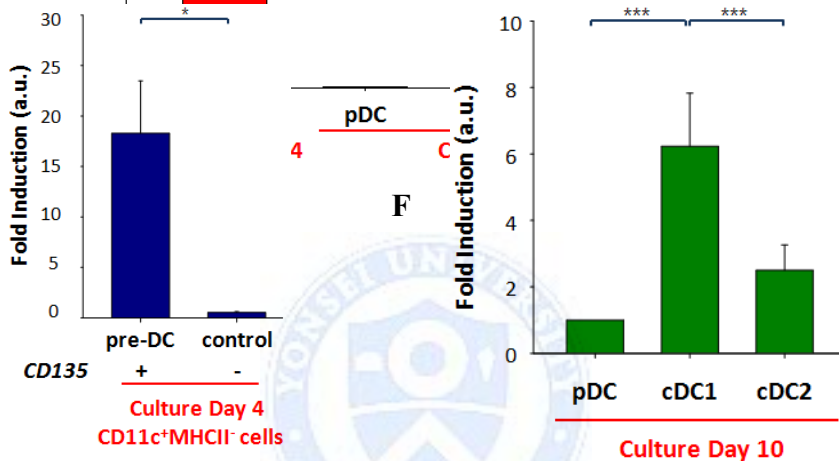
Bone marrow culture day 10 (25% Flt3L-conditioned media)



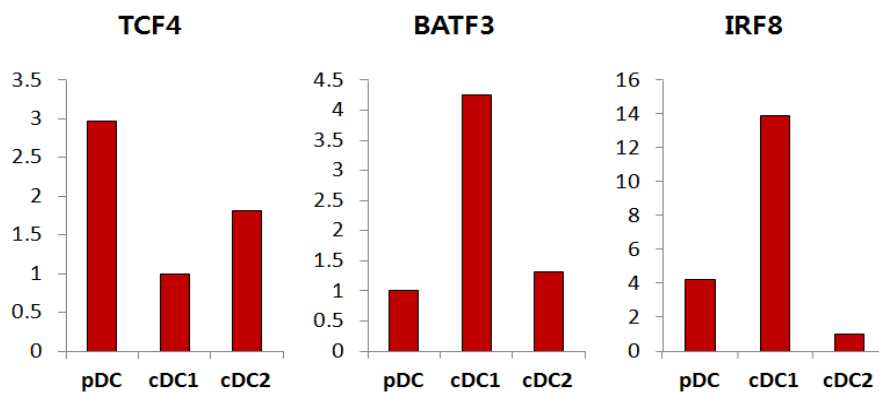
**D**



**E**



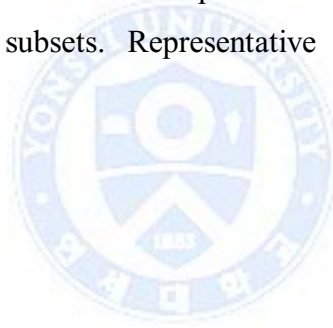
**G**



**Fig**

**ure 10. Isolation of BM DC subsets generated in vitro and miR-124**

**expression.** BM cells were cultured with 25% Flt3L-conditioned media in 12-well plates at  $1 \times 10^7$  and  $3 \times 10^6$  cells per well for preDC and matureDC analysis respectively. (A) pre-DCs were sorted as  $CD11c^+MHCII^-CD135^+$  cells on day 4.  $CD135^-$  cells were sorted for negative control. (B) pDCs were sorted as  $CD11c^+B220^+$  cells on day 10. (C) cDC1s were sorted as  $CD11c^+B220^-CD24^{hi}CD172\alpha^-$  cells and cDC2s were sorted as  $CD11c^+B220^-CD24^{int}CD172\alpha^+$  on day 10. (D) miR-124 expression of the sorted subsets was observed by real-time PCR. (E) Real-time PCR with the negative control shows that the relatively high expression of miR-124 was restricted to  $CD135^+$  pre-DCs. (F) miR-124 expression representation without pre-DC subset. (G) Real-time PCR showing the relative expression of TCF4, BATF3, and IRF8 across the sorted DC subsets. Representative data from 3 independent experiments are shown.



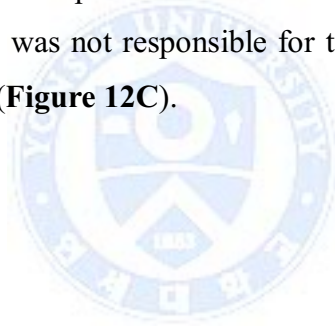
### 3.6 cDC1 cells in BM show high expression of miR-124

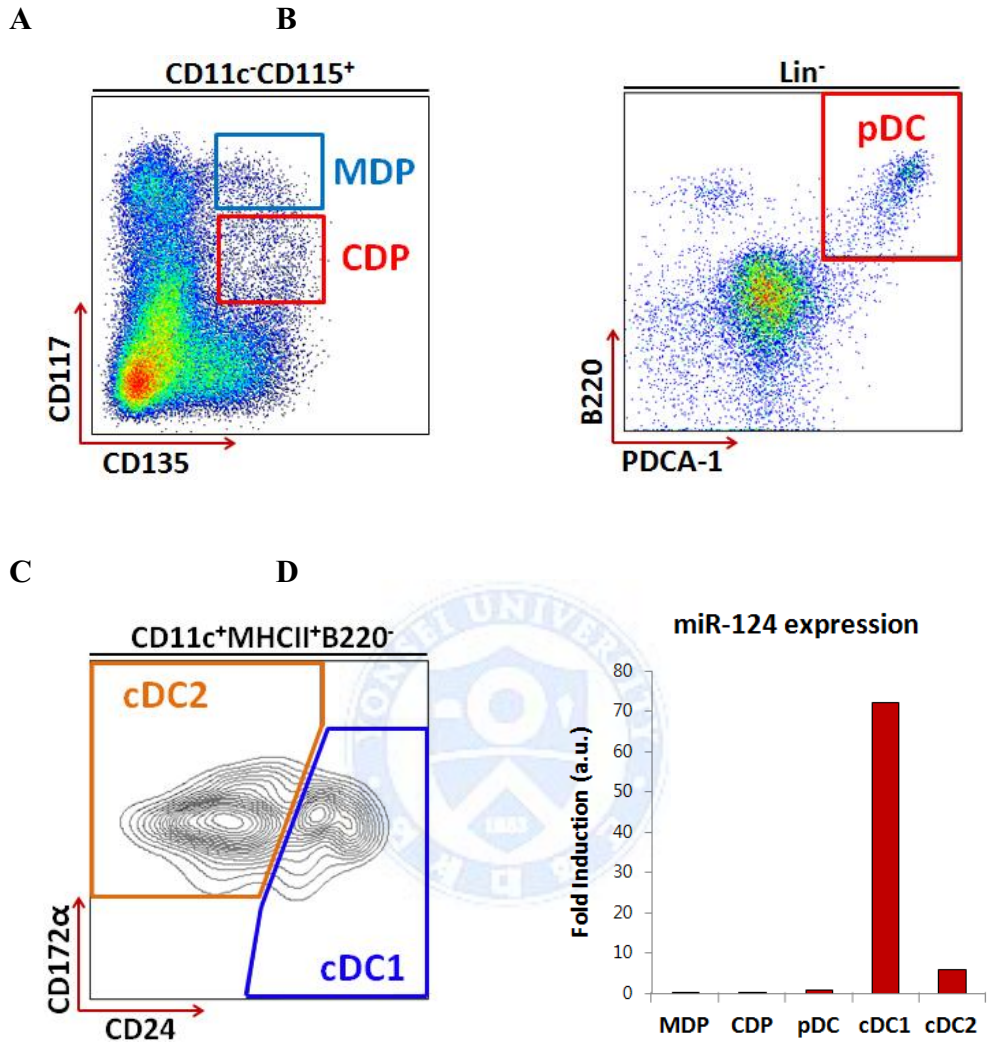
To observe miR-124 expression profiles in steady-state BM, cells were sorted from fresh BM extracted from C57BL/6 mice. Sorting strategies were formulated with similar parameters to those previously mentioned. Pre-DCs were isolated by sorting for CD11c<sup>+</sup>MHCII<sup>-</sup>CD135<sup>+</sup> from the fresh BM extraction as before. MDP and CDP progenitor cells from BM were also isolated as Lin<sup>-</sup>CD11c<sup>-</sup>CD115<sup>+</sup>CD135<sup>+</sup>CD117<sup>hi</sup> and Lin<sup>-</sup>CD11c<sup>-</sup>CD115<sup>+</sup>CD135<sup>+</sup>CD117<sup>int</sup> following previously established parameters (**Figure 11A**).<sup>16</sup> Lineage markers used for the progenitor isolation were Ly6G, CD19, Ter119, MHCII, B220, CD3, and NK1.1. pDCs were isolated as Lin<sup>-</sup>B220<sup>+</sup>PDCA-1<sup>+</sup> cells (**Figure 11B**). cDC1 and cDC2 lineages were isolated as Lin<sup>-</sup>CD11c<sup>+</sup>B220<sup>-</sup>CD24<sup>hi</sup>CD172α<sup>-</sup> and Lin<sup>-</sup>CD11c<sup>+</sup>B220<sup>-</sup>CD24<sup>int</sup>CD172α<sup>+</sup>, respectively (**Figure 11C**). Lineage markers used for matureDC isolation were Ly6G, CD19, Ter119, CD3, NK1.1, and DX5. Real-time PCR of the extracted RNA showed a relatively high expression of miR-124 in the cDC1 lineage compared to other matureDC subsets and progenitor populations (**Figure 11D**).

A difference in miR-124 profile was observed in that miR-124 was expressed highly in pre-DCs from cultured BM but not in pre-DCs from steady-state BM *in situ* (**Figure 10D**, **Figure 12B**). In a publication by Murphy *et al.*, the authors demonstrate that the pre-DC subset can be further segregated into pre-pDC/cDC2, pre-cDC1, and pre-cDC2 (nomenclature coined here).<sup>6</sup> The authors noted that CD115 and CD117 markers could be used to discriminate these pre-DC subpopulations. The cells isolated by these methods were observed to develop in a committed manner to particular matureDC subsets.<sup>6</sup> To determine whether the high relative expression of miR-

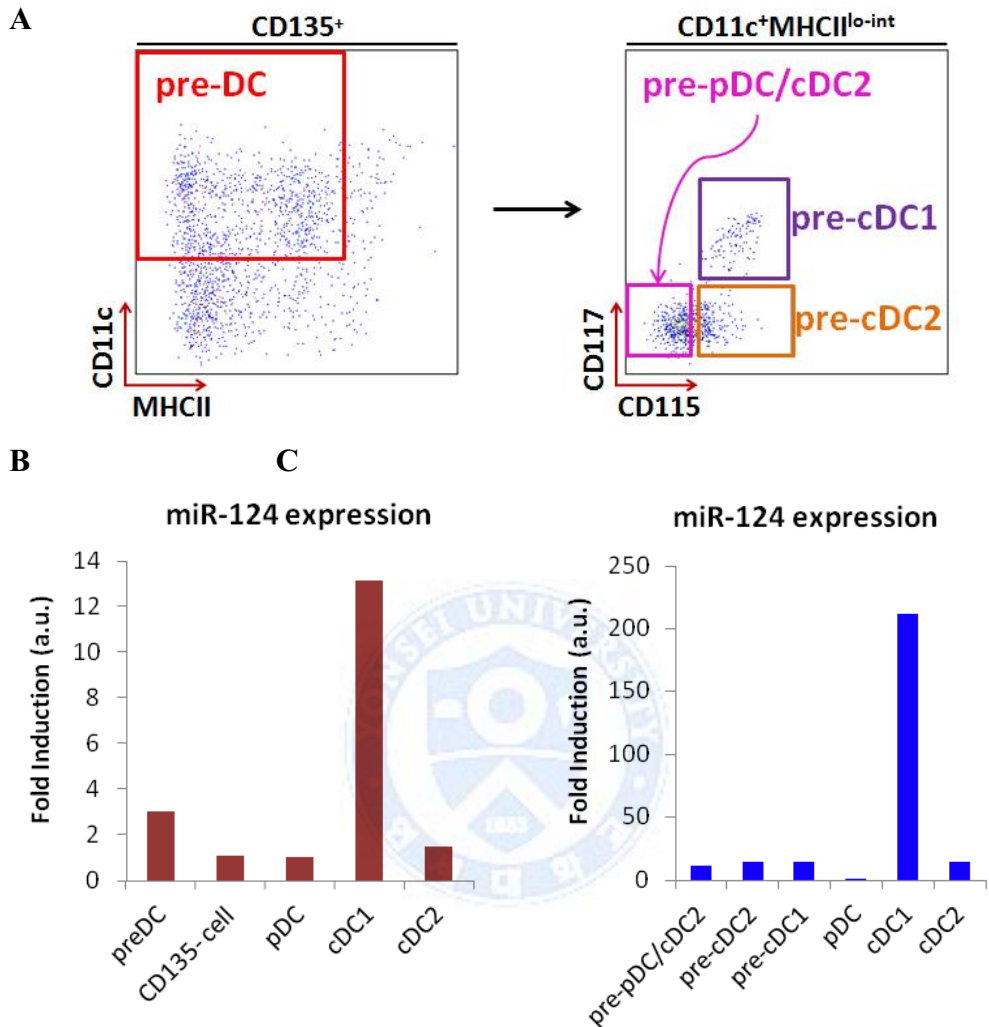


124 in cultured pre-DCs could be due to a particular pre-DC subpopulation committed to a particular matureDC subset, the three subpopulations were analyzed. The pre-DC subpopulations were all sorted for the previously described markers as  $CD11c^{+}MHCII^{lo-int}CD135^{+}$  cells. From here, pre-pDC/cDC2 was sorted as  $CD117^{-}CD115^{-}$ , pre-cDC1 was sorted as  $CD117^{+}CD115^{+}$ , and pre-cDC2 as  $CD117^{-}CD115^{+}$  (**Figure 12A**). The RNA of the sorted pre-DC subpopulations and matureDC subsets were extracted and used for real-time PCR. The cDC1 lineage showed higher expression of miR-124 than the overall pre-DC population as well as in other matureDC subsets (**Figure 12A**). All three pre-DC subpopulations showed low relative expression of miR-124 compared to cDC1 indicating that a particular subpopulation of pre-DC was not responsible for the high expression of miR-124 in cultured pre-DCs (**Figure 12C**).





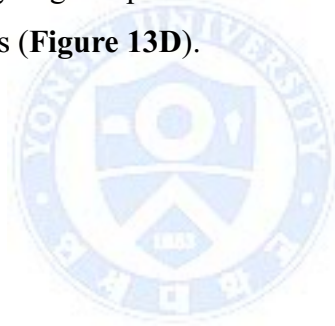
**Figure 11. Isolation of steady-state BM DC subsets and miR-124 expression.** Cells were sorted from fresh mouse BM. (A) MDPs and CDPs were sorted as  $\text{Lin}^- \text{CD11c}^- \text{CD115}^+ \text{CD135}^+ \text{CD117}^{\text{hi}}$  and  $\text{Lin}^- \text{CD11c}^- \text{CD115}^+ \text{CD135}^+ \text{CD117}^{\text{int}}$ , respectively. (B) pDCs were sorted as  $\text{Lin}^- \text{B220}^+ \text{PDCA-1}^+$ . (C) cDC1s were sorted as  $\text{Lin}^- \text{CD11c}^+ \text{MHCII}^+ \text{B220}^- \text{CD24}^{\text{hi}} \text{CD172}\alpha^-$  and cDC2s as  $\text{Lin}^- \text{CD11c}^+ \text{MHCII}^+ \text{B220}^- \text{CD24}^{\text{int}} \text{CD172}\alpha^+$ . (E) miR-124 expression in steady-state BM DC subsets.



**Figure 12. Isolation of pre-DC subpopulations in steady-state BM and miR-124 expression.** Cells were sorted from fresh BM. (A) pre-DC subpopulation sorting strategy. pre-pDC/cDC2: Lin<sup>-</sup>CD11c<sup>+</sup>MHCII<sup>lo-int</sup>CD117<sup>-</sup>CD115<sup>-</sup>. pre-cDC1: Lin<sup>-</sup>CD11c<sup>+</sup>MHCII<sup>lo-int</sup>CD117<sup>+</sup>CD115<sup>+</sup>. pre-cDC2: Lin<sup>-</sup>CD11c<sup>+</sup>MHCII<sup>lo-int</sup>CD117<sup>-</sup>CD115<sup>+</sup>. (B) miR-124 expression in pre-DC and matureDCs by real-time PCR. (C) miR-124 expression in pre-DC subpopulations and matureDCs by real-time PCR.

### 3.7 cDC1 cells in spleen show high expression of miR-124

To observe the patterns of miR-124 expression profiles in steady-state spleen, cells were sorted from fresh spleen extracted from C57BL/6 mice. Sorting strategies were formulated with similar parameters to those previously mentioned. Pre-DCs were isolated by sorting for  $\text{CD11c}^+\text{MHCII}^-\text{CD135}^+$  from the freshly extracted splenocytes (**Figure 13A**). pDCs were isolated as  $\text{Lin}^-\text{SiglecH}^+\text{B220}^+$  cells (**Figure 13B**). cDC1 and cDC2 lineages were isolated as  $\text{Lin}^-\text{CD11c}^+\text{MHCII}^+\text{B220}^-\text{CD24}^{\text{hi}}\text{CD172}\alpha^-$  and  $\text{Lin}^-\text{CD11c}^+\text{MHCII}^+\text{B220}^-\text{CD24}^{\text{int}}\text{CD172}\alpha^+$ , respectively (**Figure 13C**). Lineage markers used were: CD3, CD19, DX5, and B220. Real-time PCR of the extracted RNA from the sorted cells showed a relatively high expression of miR-124 in the cDC1 lineage compared to other subsets (**Figure 13D**).



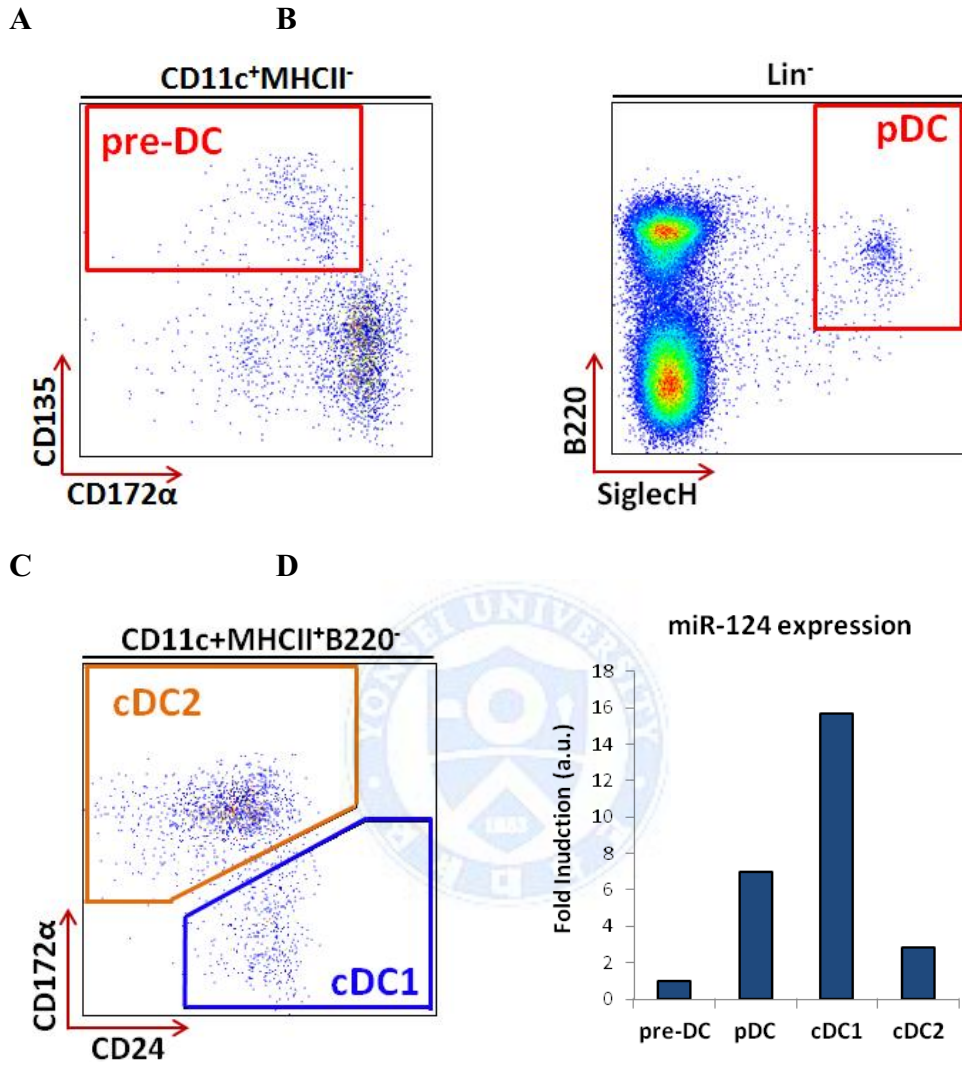


**Figure 13. Isolation of steady-state spleen DC subsets and miR-124 expression.** Cells were sorted from fresh mouse splenocytes. (A) pre-DCs were sorted as Lin<sup>-</sup>CD11c<sup>+</sup>MHCII<sup>-</sup>CD135<sup>+</sup>. (B) pDCs were sorted as Lin<sup>-</sup>SiglecH<sup>+</sup>B220<sup>+</sup>. (C) cDC1s were sorted as CD11c<sup>+</sup>B220<sup>-</sup>CD24<sup>hi</sup>CD172α<sup>-</sup> and cDC2s were sorted as CD11c<sup>+</sup>B220<sup>-</sup>CD24<sup>int</sup>CD172α<sup>+</sup>. (D) miR-124 expression of the sorted subsets was observed by real-time PCR.

### **3.8 All three miR-124 precursor transcripts contribute to miR-124 expression in cDC1 cells**

As mentioned before, miR-124 has three primary miRNA genes: pri-miR-124-1, pri-miR-124-2, and pri-miR-124-3. Three transcripts originate from these three different genes on separate chromosomes but all translate into the same mature miR-124 sequence. The map diagram detailing the origins of the precursor transcripts are shown in **Figure 14A**. Oligonucleotide probes were appropriately designed and real-time PCR was performed to determine which of the possible three precursor transcripts were expressed in DC subsets. Expression profiling in the cDC1 lineage from steady-state BM (**Figure 14B**) and steady-state spleen (**Figure 14C**) showed similar patterns of miR-124 precursor expression. Both studies showed that pri-miR-124-1 was expressed the least and pri-miR-124-3 was expressed the most but all precursors were expressed significantly within 2~3 fold of each other. The precursor miR-124 gene expressions were also measured in other DC subsets, which showed that all three genes contribute variably in different DC subsets (not shown). In other words, the definitive expression of all three miR-124 precursors indicates that they all contribute significantly to mature miR-124 expression.

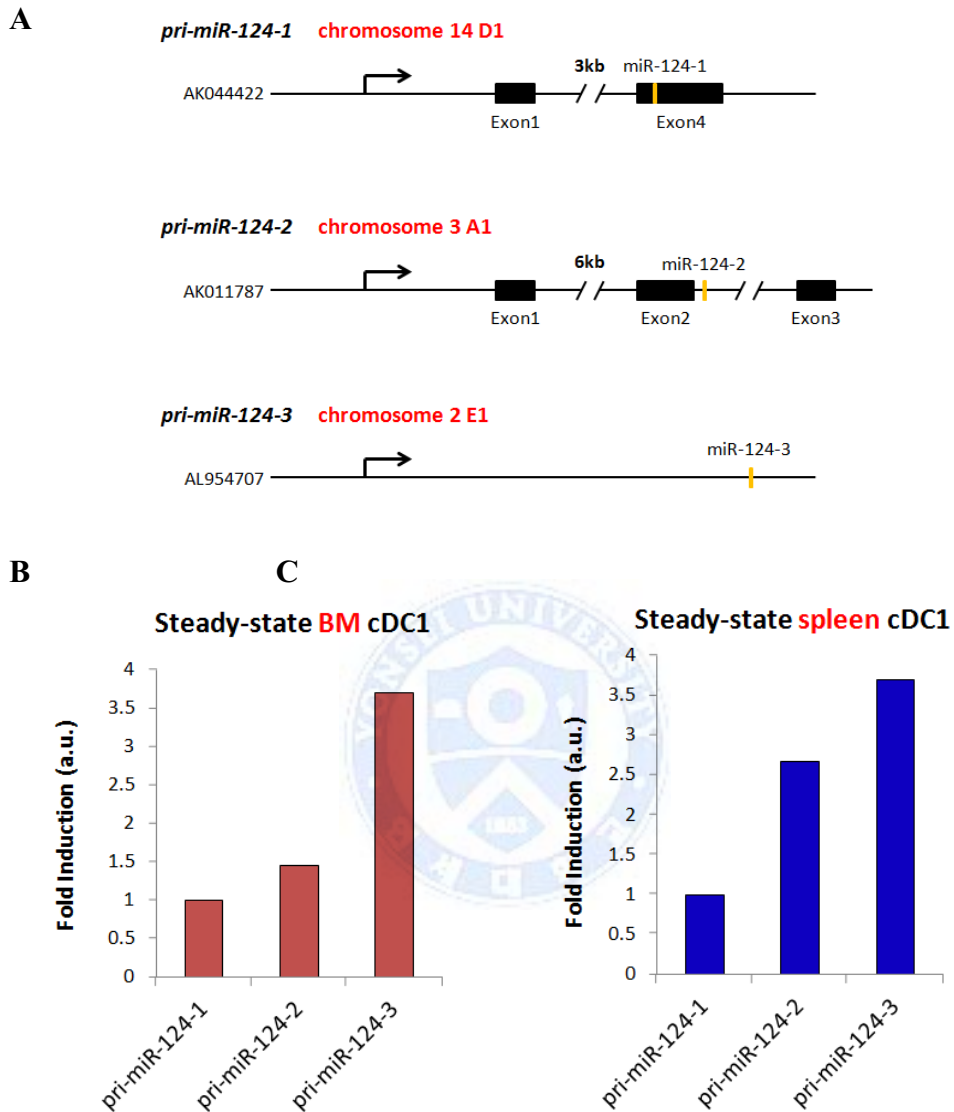


**Figure 14. Contribution of the three miR-124 precursors to miR-124 expression in DC subset.** (A) Map diagram showing the origins of the three miR-124 precursor transcripts. (B) Real-time PCR analysis showing relative miR-124 precursor expression in cDC1 cells from steady-state BM. (C) Relative miR-124 precursor expression in cDC1 cells from steady-state spleen. Representative data from 3 independent experiments are shown.



### 3.9 Overexpression of miR-124 causes significant changes to *in vitro*-cultured DC populations

Ginhoux *et al.* described an experimental apparatus where isolated BM CDPs can be re-cultured with BM filler cells and observed for developmental patterns.<sup>21</sup> BM from CD45.2 mice were extracted and sorted for CDPs. CDPs were sorted as Lin<sup>-</sup>CD115<sup>+</sup>CD135<sup>+</sup>CD117<sup>int</sup> cells as above. Ly6G, NK1.1, Ter119, MHCII, B220, CD3, CD11c, and CD19 lineage markers were used prior negative selection. The isolated CDPs were then transfected with miR-124 mimic or control mimic (cel-miR-39) before being cultured with BM filler cells extracted from CD45.1 mice in Flt3L-conditioned media. The general outline of the protocol and diagrammed in **Figure 15A**. Ginhoux *et al.* were able to observe pre-DCs derived from CD45.2 CDPs 2 days after culture and matureDCs 4 days after culture.<sup>21</sup> Cells were thus harvested 2 and 4 days post-culture and analyzed by FACS for pre-DC and matureDC subpopulations. **Figure 15B** shows the FACS analyses of CD45.2<sup>+</sup> cells transfected with miR-124 or control mimic and cultured for 4 days. Gating with matureDC markers showed no significant change in pDC development; however, there was drastic change in cDC development. There were conspicuous changes in cDC2 development. Both transfection groups showed lack of cDC1 development and also identified a previously unrecognized DC subset carrying matureDC markers. Overexpression of miR-124 seems to cause a decrease in development of this population of CD172 $\alpha$ <sup>high</sup>CD24<sup>high</sup> cells (**Figure 15B**). The transfection of miR-124 mimic into CDPs did not cause any change in pre-DC populations at day 2 of culture (data not shown). Also, transfection of miR-124 inhibitor did not induce any changes in CDP cultures (data not shown).

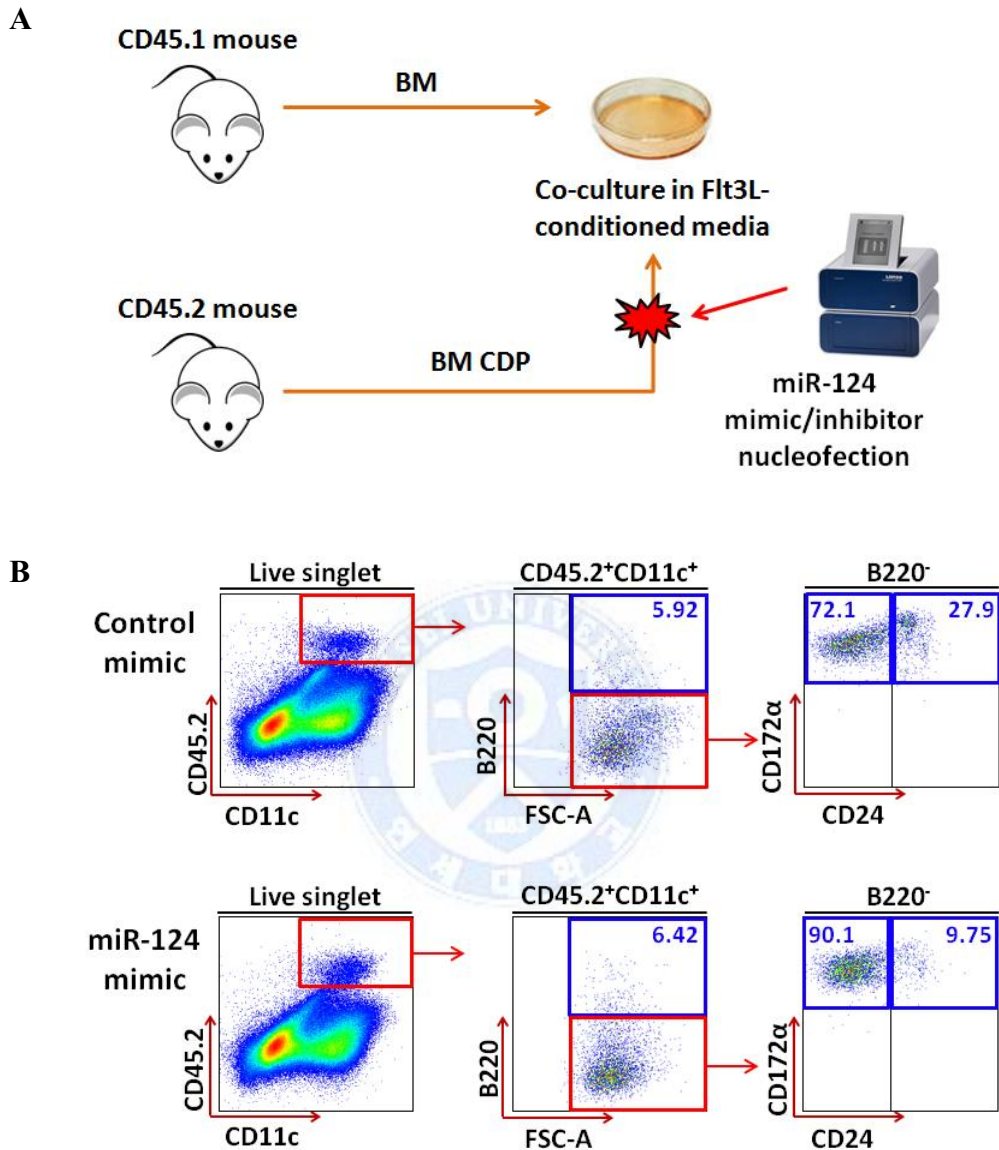


**Figure 15. Effects of miR-124 mimic transfection on DC subset development.** (A) Diagrammed protocol of mimic-transfected CDP culture experiment. (B) FACS analysis of mature DC populations derived from the transfected CDPs 4 days post-seeding. Population percentages are labeled. Representative flow cytograms from 2 independent experiments are shown.

#### IV. Discussion

MicroRNA-124 is known as the most abundant microRNA expressed in neuronal cells.<sup>2, 25</sup> Although many miRNA are starting to be linked to immunological processes, miR-124 remains unmentioned. Even in comprehensive cluster analyses of miRNA in hematopoietic and immunologic cell lines failed to recognize involvement of miR-124. Thus, the outstanding and differential expression of miR-124 in Flt3L-cultured DC populations was intriguing as it was paralleled with DC development. Since lymphoid-organ DC maintenance *in vivo* is critically dependent on Flt3L, the physiological relevance of the steady-state populations, the appropriateness of the model to study pDC and cDC origins, and the novelty of miR-124 in this context led us to focus on this initiative. This study thus aimed to critically define the dynamic profile of miR-124 in the subpopulations and delineate its interplay with relevant transcription factors that manipulate the development of particular subsets and also the functional capacities of these subsets.

Analyzing the prediction algorithm software, Tcf4 was shown to be a probable target of miR-124 while Zbtb46 was shown to be a less likely target. Symmetrical to the prediction software, the luciferase activity assay showed that miR-124 mimic binds to the inserted 3'UTR section of Tcf4. Since Tcf4 has been established to be a critical gene in the development and homeostasis of pDCs, this data suggested that miR-124 may play a major role in this process. This led us to hypothesize that miR-124 would be least expressed in pDCs, as a high expression would more effectively target Tcf4 mRNA for degradation and inhibit pDC growth. The miR-124 expression profiling of *in vitro*-generated DC subsets correlated with our hypothesis in that it was least

expressed in the pDC subset. Although, the Flt3L culture system has been established as a proficient scheme for DC investigation, it does not completely mimic *in vivo* conditions; thus it was necessary to study steady-state *in situ* conditions. Expression profiling in steady-state BM and spleen also showed least amount of miR-124 expression in the pDC subset. However, the most peculiar data was in the outstanding expression of miR-124 in cultured pre-DCs, and in cDC1 cells for steady-state conditions. There was an unexpected difference in the dynamic miR-124 expression profiles between *in vitro*-generated and steady-state *in situ* DC subpopulations. These patterns were not spontaneous and were repeated consistently in parallel trials. The drastically higher expression of miR-124 in cultured pre-DCs compared to that in mature DCs again suggested an internal switch for miR-124 activity during DC development. Meanwhile, the analysis of the pre-DC subpopulations indicates that the high expression of miR-124 in cultured pre-DCs was not due to the prevalence of a particular pre-DC subset with high miR-124 expression in Flt3L-cultured conditions. This first and foremost hinted that miR-124, like most other miRNAs, does not act on DC development one-dimensionally through a single transcription factor, but instead acts through a complex orchestra of relevant factors. In a recent publication, miR-124 was reported to be linked to the NF- $\kappa$ B pathway.<sup>7</sup> Second, these observations led us to reinvestigate our subset differentiation methods in the culture system and also consider Flt3L as a factor that may influence miR-124 expression. In light of these theories, it is though more evident that miR-124 activity is highly dynamic during DC development and indicates to an existence of purpose for such fluctuation.

Consequently, miR-124 overexpression and inhibition protocols were planned to observe the phenotypic changes of DC developmental patterns influenced by the miRNA. miR-124 knock-out mice do not currently exist as miR-124 have three precursor transcripts originating from three pri-miR-124 genes on independent chromosomes. As demonstrated, all three precursor genes also contribute in the expression of mature miR-124 in DC subsets. Currently, the triple pri-miR-124 knock-out mice does not seem to be expected to be generated in the near future.

For the present study, LNA miR-124 mimic (or inhibitor) was used with a nucleofection process in order to observe the effects of miR-124 overexpression (or inhibition). Nucleofection has been increasingly linked to efficient short nucleotide sequence transfection for infamously hard-to-transfect cells including non-adherent lymphocyte-like cells. Transfection of CDPs with this method and subsequent co-culture with filler cells in Flt3L caused a complete lack of development of the cDC1 lineage. However, this observation was observed in both miR-124 mimic and control mimic (cel-miR-39-3p) transfected cells. Cel-miR-39-3p is known to have no targets and is an established control mimic for such studies. This observation suggests that the shock process or reagents involved in nucleofection might have caused such an outcome, and this is currently being further investigated. The nucleofection process also identified a previously unrecognized DC subset with mature DC and precursor markers. The identity of this population and its relation to cDC subsets are being investigated. However, it is important to note that, miR-124 expression caused a decrease in this population. These observations were unexpected but the data gives us increasing evidence of the significant influence that miR-124 on DC development.

## V. Conclusion

miR-124 was shown to directly target the transcription factor Tcf4, which is a pivotal regulator of DC development. miR-124 was shown to be highly expressed in pre-DCs from BM cultured with Flt3L. However, in *in situ* BM and spleen at steady-state, miR-124 was shown to be most highly expressed in cDC1 cells. The dynamic expression profile of miR-124 was different between but consistent within the *in vitro*-generated DC subsets and *in situ* BM DCs. Transfection of miR-124 mimic into BM CDP followed by culture with Flt3L caused significant changes in resulting mature DC populations, where large changes in cDC1 and cDC2 lineages were observed. From our present study, the expression of miR-124 identified previously unrecognized DC subsets carrying DC markers of mature and precursor states, which is being further investigated. These observations suggest that miR-124 plays an important and mechanistic role in the development of DC subsets.

## References

- 1 J. Agudo, A. Ruzo, N. Tung, H. Salmon, M. Leboeuf, D. Hashimoto, C. Becker, L. A. Garrett-Sinha, A. Baccarini, M. Merad, and B. D. Brown, 'The Mir-126-Vegfr2 Axis Controls the Innate Response to Pathogen-Associated Nucleic Acids', *Nat Immunol*, 15 (2014), 54-62.
- 2 M. L. Baudet, K. H. Zivraj, C. Abreu-Goodger, A. Muldal, J. Armisen, C. Blenkiron, L. D. Goldstein, E. A. Miska, and C. E. Holt, 'Mir-124 Acts through Corest to Control Onset of Sema3a Sensitivity in Navigating Retinal Growth Cones', *Nat Neurosci*, 15 (2012), 29-38.
- 3 B. Cisse, M. L. Caton, M. Lehner, T. Maeda, S. Scheu, R. Locksley, D. Holmberg, C. Zweier, N. S. den Hollander, S. G. Kant, W. Holter, A. Rauch, Y. Zhuang, and B. Reizis, 'Transcription Factor E2-2 Is an Essential and Specific Regulator of Plasmacytoid Dendritic Cell Development', *Cell*, 135 (2008), 37-48.
- 4 D. Dudziak, A. O. Kamphorst, G. F. Heidkamp, V. R. Buchholz, C. Trumpfheller, S. Yamazaki, C. Cheong, K. Liu, H. W. Lee, C. G. Park, R. M. Steinman, and M. C. Nussenzweig, 'Differential Antigen Processing by Dendritic Cell Subsets in Vivo', *Science*, 315 (2007), 107-11.
- 5 I. Dunand-Sauthier, M. L. Santiago-Raber, L. Capponi, C. E. Vejnár, O. Schaad, M. Irla, Q. Seguin-Estevez, P. Descombes, E. M. Zdobnov, H. Acha-Orbea, and W. Reith, 'Silencing of C-Fos Expression by MicroRNA-155 Is Critical for Dendritic Cell Maturation and Function', *Blood*, 117 (2011), 4490-500.
- 6 G. E. Grajales-Reyes, A. Iwata, J. Albring, X. Wu, R. Tussiwand, W. Kc, N. M. Kretzer, C. G. Briseno, V. Durai, P. Bagadia, M. Haldar, J. Schonheit, F. Rosenbauer, T. L. Murphy, and K. M. Murphy, 'Batf3 Maintains Autoactivation of Irf8 for Commitment of a Cd8alpha(+) Conventional Dc Clonogenic Progenitor', *Nat Immunol*, 16 (2015), 708-17.
- 7 D. Jeong, J. Kim, J. Nam, H. Sun, Y. H. Lee, T. J. Lee, R. C. Aguiar, and S. W. Kim, 'MicroRNA-124 Links P53 to the Nf-Kappab Pathway in B-Cell Lymphomas', *Leukemia*, 29 (2015), 1868-74.



- 8 T. M. Johanson, M. Cmero, J. Wettenhall, A. M. Lew, Y. Zhan, and M. M. Chong, 'A MicroRNA Expression Atlas of Mouse Dendritic Cell Development', *Immunol Cell Biol* (2014).
- 9 T. M. Johanson, J. P. Skinner, A. Kumar, Y. Zhan, A. M. Lew, and M. M. Chong, 'The Role of MicroRNAs in Lymphopoiesis', *Int J Hematol*, 100 (2014), 246-53.
- 10 J. J. Karrich, L. C. Jachimowski, M. Libouban, A. Iyer, K. Brandwijk, E. W. Taanman-Kueter, M. Nagasawa, E. C. de Jong, C. H. Uittenbogaart, and B. Blom, 'MicroRNA-146a Regulates Survival and Maturation of Human Plasmacytoid Dendritic Cells', *Blood*, 122 (2013), 3001-9.
- 11 D. Kingston, M. A. Schmid, N. Onai, A. Obata-Onai, D. Baumjohann, and M. G. Manz, 'The Concerted Action of Gm-CSF and Flt3-Ligand on in Vivo Dendritic Cell Homeostasis', *Blood*, 114 (2009), 835-43.
- 12 K. Liu, G. D. Victora, T. A. Schwickert, P. Guernonprez, M. M. Meredith, K. Yao, F. F. Chu, G. J. Randolph, A. Y. Rudensky, and M. Nussenzweig, 'In Vivo Analysis of Dendritic Cell Development and Homeostasis', *Science*, 324 (2009), 392-7.
- 13 A. Mildner, E. Chapnik, O. Manor, S. Yona, K. W. Kim, T. Aycheh, D. Varol, G. Beck, Z. B. Itzhaki, E. Feldmesser, I. Amit, E. Hornstein, and S. Jung, 'Mononuclear Phagocyte Mirnome Analysis Identifies Mir-142 as Critical Regulator of Murine Dendritic Cell Homeostasis', *Blood*, 121 (2013), 1016-27.
- 14 A. Mildner, and S. Jung, 'Development and Function of Dendritic Cell Subsets', *Immunity*, 40 (2014), 642-56.
- 15 K. M. Murphy, 'Transcriptional Control of Dendritic Cell Development', *Adv Immunol*, 120 (2013), 239-67.
- 16 S. H. Naik, P. Sathe, H. Y. Park, D. Metcalf, A. I. Proietto, A. Dakic, S. Carotta, M. O'Keeffe, M. Bahlo, A. Papenfuss, J. Y. Kwak, L. Wu, and K. Shortman, 'Development of Plasmacytoid and Conventional Dendritic Cell Subtypes from Single Precursor Cells Derived in Vitro and in Vivo', *Nat Immunol*, 8 (2007), 1217-26.
- 17 N. Onai, K. Kurabayashi, M. Hosoi-Amaiike, N. Toyama-Sorimachi, K.

- Matsushima, K. Inaba, and T. Ohteki, 'A Clonogenic Progenitor with Prominent Plasmacytoid Dendritic Cell Developmental Potential', *Immunity*, 38 (2013), 943-57.
- 18 H. Park, X. Huang, C. Lu, M. S. Cairo, and X. Zhou, 'MicroRNA-146a and MicroRNA-146b Regulate Human Dendritic Cell Apoptosis and Cytokine Production by Targeting Traf6 and Irak1 Proteins', *J Biol Chem*, 290 (2015), 2831-41.
- 19 S. H. Park, C. Cheong, J. Idoyaga, J. Y. Kim, J. H. Choi, Y. Do, H. Lee, J. H. Jo, Y. S. Oh, W. Im, R. M. Steinman, and C. G. Park, 'Generation and Application of New Rat Monoclonal Antibodies against Synthetic Flag and Ollas Tags for Improved Immunodetection', *J Immunol Methods*, 331 (2008), 27-38.
- 20 A. Schlitzer, J. Loschko, K. Mair, R. Vogelmann, L. Henkel, H. Einwachter, M. Schiemann, J. H. Niess, W. Reindl, and A. Krug, 'Identification of Ccr9-Murine Plasmacytoid Dc Precursors with Plasticity to Differentiate into Conventional Dcs', *Blood*, 117 (2011), 6562-70.
- 21 A. Schlitzer, V. Sivakamasundari, J. Chen, H. R. Sumatoh, J. Schreuder, J. Lum, B. Malleret, S. Zhang, A. Larbi, F. Zolezzi, L. Renia, M. Poidinger, S. Naik, E. W. Newell, P. Robson, and F. Ginhoux, 'Identification of Cdc1- and Cdc2-Committed Dc Progenitors Reveals Early Lineage Priming at the Common Dc Progenitor Stage in the Bone Marrow', *Nat Immunol*, 16 (2015), 718-28.
- 22 K. Shortman, and Y. J. Liu, 'Mouse and Human Dendritic Cell Subtypes', *Nat Rev Immunol*, 2 (2002), 151-61.
- 23 L. A. Smyth, D. A. Boardman, S. L. Tung, R. Lechler, and G. Lombardi, 'MicroRNAs Affect Dendritic Cell Function and Phenotype', *Immunology*, 144 (2015), 197-205.
- 24 X. Su, C. Qian, Q. Zhang, J. Hou, Y. Gu, Y. Han, Y. Chen, M. Jiang, and X. Cao, 'Mirnomes of Haematopoietic Stem Cells and Dendritic Cells Identify Mir-30b as a Regulator of Notch1', *Nat Commun*, 4 (2013), 2903.
- 25 A. J. Svahn, J. Giacomotto, M. B. Graeber, S. Rinkwitz, and T. S. Becker, 'Mir-124 Contributes to the Functional Maturity of Microglia', *Dev Neurobiol* (2015).

## 수지상 세포의 분화에 따라 조절되는 microRNA 의 분석

<지도교수 박채규>

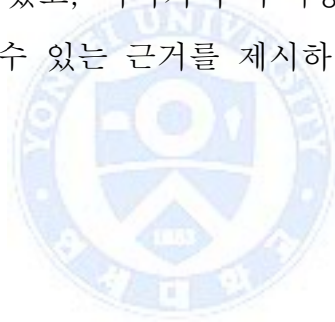
연세대학교 대학원 의과학과

한선

### Abstract

수지상세포(dendritic cells, DCs)는 항원 특이적인 T세포 반응을 유도하는 전문화된 항원제시세포로서 cDC1과 cDC2로 세분화되는 classical 수지상세포(cDC)와 plasmacytoid 수지상세포(pDC) 등 다양한 아형이 존재한다. 수지상세포 아형에 특이적으로 발현되는 전사인자에 대한 연구는 다수 보고되었으나, 수지상세포 분화 과정에 관여하는 전사인자들의 발현을 조절하는 정확한 기전에 대한 연구는 아직 미비하다. microRNA(miRNA)는 체내 여러 유전자의 발현을 전사후 과정에서 조절하는 중추적인 조절인자로 알려져 있으나 면역계에서의 역할과 작용에 대한 연구는 부족하다. 본 연구자는 수지상세포의 발달과 기능 형성에 관여하는 miRNA를 찾고자 수지상세포의 발달과 연관성이 있는 전사인자들의 3'UTR을 표적으로 하는 miRNA를 스크리닝하였다. 이를 통해 pDC의 분화와 기능에 관여하는 전사인자 Tcf4의 3'UTR이 miR-124의 표적이 될 수 있음을 확인하였다. In vitro에서 마우스 골수세포를 Flt3L와 함께 배양한 후 수지상세포의 아형들을 분리하여 qPCR로 확인한 결과 cDC의 전구

세포에서 miR-124가 현저히 높게 발현하는 것을 관찰하였다. 배양하지 않은 마우스 골수에서는 수지상세포의 전구세포, pDC 및 CD172a<sup>+</sup> cDC2 보다 CD24<sup>+</sup> cDC1에서 miR-124의 발현이 높게 나타났다. 수지상세포의 분화 과정에서 miR-124가 어떠한 작용을 하는지 확인하기 위하여 miR-124의 mimic 또는 억제제를 마우스 골수에서 분리한 수지상세포 공통전구체(common DC progenitor, CDP)에 transfection한 후 Flt3L와 함께 배양하였다. 그 결과 기존에 보고된 바 없는 수지상세포 아형의 숫자가 크게 감소하는 것을 발견하였다. 본 연구를 통하여 miR-124가 수지상세포의 분화 과정 이전에 관여하는 것을 확인하였고, 나아가서 수지상세포의 복잡한 분화 과정을 더 깊이 이해할 수 있는 근거를 제시하였다.



---

핵심되는 말: 수지상세포, microRNA, 아형, 분화, Flt3L, 전사후 조절

## Publication List

1. S. Lee, S. Lim, O. Ham, S.Y. Lee, K. C. Hwang, *et al.*,  
‘ROS-mediated Bidirectional Regulation of MiRNA Results  
in Distinct Pathologic Heart Conditions.’ *Biochem Biophys  
Res Commun.* 465(2015):349-55.

